Locating park-and-ride facilities for resilient on-demand urban mobility

Elise Henry, Angelo Furno, Nour-Eddin El Faouzi, David Rey

Version of Record: https://www.sciencedirect.com/science/article/pii/S136655452100315X
Manuscript_ac6c7820a126cffeb71450e9a1a310be

Locating park-and-ride facilities for resilient on-demand urban mobility

Elise Henry[a,*], Angelo Furno[a], Nour-Eddin El Faouzi[a] and David Rey[b]

[a] Univ. of Lyon, Univ. Gustave Eiffel, ENTPE, LICIT UMR_T9401, F-69675, Lyon, France
[b] SKEMA Business School, Université Côte d'Azur, Sophia Antipolis Campus, France

ARTICLE INFO

Keywords:
Park-and-ride
On-demand mobility
Resilience
Mixed-integer programming
Lagrangian relaxation

ABSTRACT

Urban transport networks, yet essential, are frequently impacted by recurrent disruptions such as public transport failures, adverse weather or strikes. Flexible transit systems can be used to limit the impacts of recurrent disruptions on urban mobility. In this study, we examine the potential of on-demand park-and-ride systems to complement an existing transport infrastructure and improve network resilience. We formulate a stochastic park-and-ride facility location problem which captures the entire user trip chain from the origin to the destination via pick up and drop off nodes in a mobility network. We use a Logit model to capture users' mode choice between paths in the park-and-ride system and a reserve travel option. Stochastic scenarios are used to represent varying traffic conditions to recurrent disruptions. The goal is to maximize the expected ridership in the park-and-ride system by identifying the optimal location of pick up and drop off facilities and accounting for users' mode choice. We develop a customized Lagrangian relaxation algorithm to solve the resulting mixed-integer programming problem on large scale instances and quantify its performance through a sensitivity analysis by comparing it against a direct mixed-integer linear programming approach. Numerical results are presented on realistic instances generated based on the city of Lyon, France. Our findings show that the proposed methodology can provide key insights to support the deployment of park-and-ride systems and improve network resilience by capturing a significant proportion of users under disrupted traffic conditions.

1. Introduction

Transportation networks are subject to many disruptions which may affect their performances, typically already sensitive to varying mobility demands. The concept of park-and-ride (P&R) appeared in the 1930s in the United States (Noel, 1988) and quickly emerged globally as a means to improve traffic conditions in urban areas. P&R systems have the potential to attract car users by providing benefits such as congestion relief, environmental preservation, transportation cost reduction, as discussed for instance by Parkhurst (1995). By incentivizing modal shift from private cars to higher occupancy vehicles, P&R may help in mitigating urban congestion and reducing pollution effects. Annisa et al. (2019) discuss in the benefits of such a P&R system in Bandung City, Indonesia, for air emissions and congestion but highlight the importance of having an adequate public transportation management system. Furthermore, mobility networks face recurrent disruptions that affect network performance and ridership. For example, significant adverse weather, *e.g.*, heavy rain/snow, pollution peaks, road network maintenance operations and special events, *e.g.*, sports and entertainment, may reduce network capacity and/or affect travel demand patterns (Gauthier et al., 2018; Zhu et al., 2016; Donovan and Work, 2017; Lu et al., 2016; Bíl et al., 2015). By reducing the number of private vehicles, shared-mobility systems, such as P&R, aim at improving the traffic conditions. According to Sun (2017), shared mobility increases traffic efficiency and reduces unnecessary external costs such as greenhouse gas emission, mainly caused by low average occupancy.

In this study, we consider a P&R facility location problem which captures users' entire trip chains – including access, transit and egress trips – in an urban mobility network. More specifically, we aim to identify the optimal locations for pick up and drop off services in the P&R system to maximize the expected ridership under both normal network traffic conditions and recurrent disruptions which regularly negatively affect traffic conditions. In this context, a low computation time appears as an additional requirement towards rapidly proposing a fitted solution for localized recurrent disturbances, which might unequally and unpredictably impact the accessibility of the mobility network and its performance. In this study, we attempt to quantify the attractiveness of the P&R system by modeling users' mode choice model and seek to maximize the expected ridership within the P&R system at the expense of users' reserve travel option. The proposed solution builds on and significantly extends the approach of Aros-Vera et al. (2013) where the authors only focused on the pick up and transit part of users' trip, thus ignoring the impact of drop off location with

ORCID(s):

respect to to the final destination. We address this gap by modeling both pick up and drop off locations, thus capturing the entire trip chain of a P&R user in the mobility network.

In our study, the proposed P&R system consists of a shuttle service that complements the existing mobility network. We capture the mobility of user's outside of our P&R system through the reserve mode representing the private travels. Through our methodology, we aim at providing the optimal locations for the pick ups and the drop offs and the optimal pick up/drop off combination in terms of travel time for a given origin/destination, helpful to deploy an on-demand shuttle service. Both decisions are adapted to recurrent disruptions such as public transport failures or snowfall, with the aim of increasing the ridership of the proposed P&R system. To that purpose, we aim at determining the optimal locations for: *i)* the pick ups, *i.e.*, the car parks where commuters can transfer from their personal vehicle to shared mobility solutions (*e.g.*, shuttle buses); and *ii)* the drop offs, *i.e.*, the transit stops where users exit the P&R system and continue to their destination by other means, such as walking, micro-mobility (*e.g.*, bike-sharing, e-scooters) solutions or the regular public transportation. We assume a given budget constraint for the constructions of the car parks and transit stops. We use a multinomial logit choice model to determine the proportion of people using the P&R system and aim to maximize the expected P&R ridership.

The main contributions of our study are: *i)* the mathematical formulation of an integrated P&R system which captures the entire user trip chain from the origin to the destination via pick up and drop off nodes in a mobility network and accounting for mode choice; *ii)* the incorporation of a stochastic programming approach to take into account recurrent disruptions in an urban mobility network; *iii)* the development of a customized Lagrangian Relaxation Algorithm (LRA) able to provide competitive solutions, by out-performing commercial MILP solver CPLEX based on a branch-and-cut search, for large-scale mobility networks in a restricted computational time; *iv)* the implementation of the proposed P&R system on a realistic instance representing the city of Lyon, France, which provides key insights for mobility service providers in urban areas.

The rest of the paper is organized as follows. Section 2 discusses the literature review. Section 3 describes the problem (Sec. 3.1), presents the mathematical notations (Sec. 3.2) and the mode-choice (Sec. 3.3) model, sets the constraints (Sec. 3.4) as well as the objective function (Sec. 5a) and formulates the problem (Sec. 3.6). Section 4 presents the LRA used to solve large-scale instances. In Section 5, we present the data we used to experiment our problem. The presentation of the results obtained through our model is provided in Section 6. We first discuss about the performance of our model solved with the MILP approach and with our developed algorithm through a sensitivity analysis depending on the graph size and on a set of different parameters (Sec. 6.1), and then present the results on a real case study (Sec. 6.2). Conclusions and future works are discussed in Section 7.

2. Literature review

Several studies explore the implementation of shared mobility services in cities with the aim to improve urban transportation systems. Such approaches typically fall within the broad field of transit network design. Our focus is on the design of on-demand mobility services, in opposition to traditional transit systems, *e.g.*, fixed-schedule, fixed routes, to improve the resilience of the urban transport system with respect to recurrent disruptions. Accordingly, in our review of the literature, we first examine studies which proposed on-demand transit systems (Sec. 2.1). We then review studies which addressed the resilience of mobility networks (Sec. 2.2) before outlining our contributions.

2.1. On-demand transit systems

According to Machado et al. (2018), "shared mobility can be defined as trip alternatives that aim to maximize the utilization of the mobility resources that a society can pragmatically afford, disconnecting their usage from ownership". Farahani et al. (2010) notice that "facility location can be considered a one-hundred year old science". Such issues are part of P&R problems which aims at optimally locating the car parks by taking several kinds of constraints into account. Danach et al. (2019) developed an algorithm based on the Lagrangian Relaxation to solve a variant of the hub location routing problems where each cluster of spoke nodes allocated to a hub constitutes a directed route that starts from the hub, visits all the spokes in the same cluster, and terminates to the same hub. The minimization of the travel cost such as travel time should be one of them. Song et al. (2017) aim at minimizing the travel time and the expected waiting time experienced by transit users by modeling transit service frequency and accounting for user equilibrium in the optimization of the location and capacity of park-and-ride facilities. Lee and Nair (2021) tend to improve the journey times by determining a set of fixed routes both based on the demand, estimated with mobile phone data under normal conditions and supposed to be all served by the new transport mode, and the problem's structure through a

bi-level programming.

Another objective should be to maximize the ridership of P&R systems. Farhan and Murray (2008) aim to maximize P&R demand coverage but also the accessibility and the integration with existing transit systems by minimizing the park distance to the major roads of the network. Discrete choice models can be used to estimate modal shift in mobility networks and the ridership within the transportation system. Aros-Vera et al. (2013) propose to maximize the ridership within a P&R system by optimally locating a given number of parks used to access a shared mobility service. The authors capture mode choice decisions via a logit model wherein users' disutilities represent their generalized travel costs via the designed P&R system and private travel is a reserve option. Chen et al. (2016) and Chen and Kim (2018) propose a combined mode split and traffic assignment model to find the combination of possible locations and capacity for the P&R system of interest. Cavadas and Antunes (2019) aim at diminishing the number of cars in urban areas by deploying P&R facilities and adopting a fixed travel cost logit-based model to capture demand elasticity. In their iterative approach to design a transport network with a variable travel demand, Lee and Vuchic (2005) aim at determining the transit network frequency, through a logit formulation based on the the travel cost including the travel time. The approach tends to both minimizing travel time and social cost and maximizing the profit. According to the Mohring effect (Mohring, 1972), an increase in travel demand may lead to more efficient transit networks if service frequency is increased due to reduced user waiting time. Du and Wang (2014) propose a continuum model, able to incorporate commuter heterogeneity and travel time reliability, to optimally develop multiple P&R services, by defining the optimal transit locations, in a linear travel corridor with competitive railway/highway system. Along a corridor with continuous entry points to the highway, railway and continuous P&R transfer services, the commuters could use the private vehicle, the railway to the P&R mode to reach the destination. The multimodal choice is based on the user equilibrium that a commuter would use the travel mode with the lower generalized travel cost.

Basciftci and Van Hentenryck (2020) design an on-demand multimodal transit system through a bi-level optimization process, considering the latent demand as a pool of potential riders with a personalized mode choice model, deciding whether a rider will switch mode for a given on demand transit system. The model aims at finding the most cost-efficient and convenient route for each trip with the inclusion of a personalized mode choice for each rider to determine mode switching or latent demand. The designed transit network optimizes the hubs locations for connecting them with high frequency buses and each rider chooses the optimal route under a given design through buses. To determine a time-varying demand adapted fleet of vehicles, Zhang et al. (2021) proposes a two-stage heuristic approach for solving the fleet management problem under time-varying demand by first optimizing the vehicles' utilization schedule and second optimizing the vehicle purchase and retirement schedules. Finally, Ruan et al. (2016) consider a P&R facility location problem adapted to a specific event, the International Horticultural Exposition 2019, Beijing, China, by both minimizing the total travel cost and maximizing the accessibility for all the passengers during the special event subject to a given total construction budget and the availability of candidate locations.

Although the optimal location of P&R facilities has received considerable attention in the literature, the focus has been on developing formulations that account for long-term user behavior. This presumes that the deployment of P&R facilities and the network design is permanent, whereas we aim at developing a flexible P&R system where connections between facilities can be adjusted based on network disruptions. We focus on the case of re-configurable P&R facilities which are designed to improve network resilience by offering an on-demand mobility service complementary to the existing transport network.

2.2. Quantifying and improving the resilience of mobility networks

Transportation networks are frequently subject to various types of disruptions such as extreme weather events, human attacks or technological failures. This may affect the performance of transportation systems which are essential for societies hence the interest of obtaining a resilient transport system. Holling (1973) first introduced this concept in ecological systems and defined it as "the ability of these systems to absorb changes of state variables, driving variables, and parameters, and still persist". In the field of transportation, two major approaches, the topological and the dynamic ones, are studied to analyse the transport network resilience to ensure acceptable levels of service under disrupted network conditions (Haimes, 2009; Hassan et al., 2019).

The topological approach, based on the graph theory aims at quantifying the resilience looking at the connectivity properties of the network, using centrality measures. The transport network is represented by an undirected or directed graph $G = (V, E)$, where edges (E) correspond to roads, and nodes (N) to intersections. Such approach is mainly used. Freiria et al. (2015) identified the most important roads in a Portuguese network thanks to patterns. Shalaby et al. (2016) studied performances of public transport network in Toronto and USA. Tu et al. (2010) applied topologi-

cal vulnerability index, inter alia, on Sioux Falls network (Berche et al., 2009). Graph theory is "suitable for identifying structural criticalities" (Eusgeld et al., 2009). By randomly or targetly removing some nodes or edges, the impact of an event influencing the transport network could be quantified. The dynamic approaches are closer to the traffic theory. They characterize resilience by taking into account actual or simulated traffic dynamics, using demand-sensitive indicators like links speed, queue length, road capacity or recovery time, as discussed in (Murray-Tuite, 2006; Oliveira et al., 2014). Jenelius and Cats (2015) notice that increasing the public transport network contribute to greater capability to withstand system breakdowns, by increasing the network redundancy. Following the topological approach used to quantify the network resilience, in the context of graph augmentation and centrality improvement, Bergamini et al. (2018) and Angelo et al. (2016) suggest to maximize the Edge Betweenness Centrality measure through an optimization problem by creating a limited set of edges. Crescenzi et al. (2016) consider a similar optimization problem by quantifying how much a node can increase its Node Closeness Centrality measure with a graph augmentation. However, it is worth to mention that these approaches are extremely time consuming and therefore hardly apply to the settings of our study that focus on large metropolitan areas by also taking into account traffic dynamics as described in terms of travel demand and travel times (Gauthier et al., 2018).

The deployment of relief trains to enhance the resilience level of the rail network by optimizing location and allocation of them is examined by Bababeik et al. (2018). The authors propose a bi-objective location and allocation model for relief trains in the rail network with the aim of maximizing the cooperative coverage of link importance by relief trains stations and minimizing the total travel time from relief trains stations to the whole components of the network. Finally, Henry et al. (2021) proposed a flexible transit network design methodology by deploying a reconfigurable shuttle service, adapted to some recurrent disruptions such as weather events or public transport failures.

In this study, we build on and significantly extend the methodology developed by Aros-Vera et al. (2013) which aims to maximize the ridership of a public transport system via modal shift. In their study, Aros-Vera et al. considered paths subdivided in two portions: from the origin to a P&R facility and from the P&R facility to the public transport station considered as a central business district. In our study, we model paths from users' origin to their destinations by considering three portions: from the origin to a P&R facility (pick up), from the pick up facility to another P&R facility (drop off),and from the drop off facility to the final destination. This extension of two links to three links is non-trivial since it requires additional modeling and significantly increases the size of the optimization problems at hand. Since some of the disruptions are recurrent such as public transport failures, strikes, or heavy rainfalls and snowfalls, user behavior is predictable and can be captured by scenario-specific travel demand trip tables. For these reasons, we choose to elaborate a stochastic problem, rather than a deterministic one, in order to consider both normal traffic conditions and recurrent disruptions in the deployment of the transport service. To solve large scale problems, we develop a Lagrangian Relaxation Algorithm (LRA) which aims at simplifying a model by relaxing some constraints. We next present the proposed methodology.

3. Park-and-ride facility location problem

In this section, we focus on the presentation and the formulation of the proposed P&R facility location problem. After describing the problem (Sec. 3.1), we present the mathematical notations used in the rest of the paper (Sec. 3.2), we introduce the mode choice model (Sec. 3.3) and we formulate the constraints (Sec. 3.4) and the objective function (Sec. 3.5). Finally we summarize the mixed-integer programming formulation of the proposed P&R facility location problem (Sec. 3.6).

3.1. Problem description

We consider the problem of deploying a P&R system in an urban mobility network. We assume that there is a known travel demand for a set of origin-destination pairs in the network. We consider two travel mode choices, the proposed P&R system and the reserve mode, which represents user's private mode choice. As previously explained, the P&R system to be designed consists of pick up location, where users can park their private vehicles and board transit shuttles, and drop off location, where users disembark and are assumed to pursue their journey by walking to their destination. To be attractive, a P&R system must provide competitive travel times compared to users' reserve mode. We propose to capture users' mode choice between using the P&R system and their reserve mode via a discrete choice model. To maximize the P&R attractiveness, car parks (pick ups) should be within short driving range from users' origins, and transit stops (drop offs) should be in close walking distance to users' destinations. To put it in a

nutshell, the goal of the P&R facility location problem is to determine the optimal locations for pick ups and drop offs so as to maximize ridership in the P&R system. Observe that the roles of pick up and drop off nodes is only indicative. In principle, a P&R transit stop can serve both purposes, *i.e.*, pick up or drop off.

3.2. Mathematical modeling framework

In this article, we propose a stochastic problem which aims at considering a set Ω of different scenarios ω with a probability of occurrence p^{ω}, representing both normal conditions or recurrent disruptions, to optimize our P&R system in an existing transport network. The stochastic nature of the problem allows making resilient-aware P&R design, by taking into account the probability of occurrence of multiple possible scenarios of disruptions. The scenario-dependency of the following variables and parameters will be noted with a superscript $^{\omega}$. The transport network is represented by a directed graph with E edges representing the roads and N nodes corresponding to the road intersections. In each scenario we determine the set of the OD pairs (r, s) with a non-zeros total travel demand d^{ω}_{rs}. This set is called $W^{\omega} = \{(r, s) : d^{\omega}_{rs} > 0, r \in N, s \in N\}$.

For each OD pair, we determine the sets of the accessible pick ups i and drop offs j. To be attractive, we assume that the generic P&R pick up i has to be reached from the origin r in a reasonable time t^{ω}_{ri} lower than a fixed time t^{access}, as well as the destination s must be reached from the drop off j in a given time t^{ω}_{js} lower than the fixed egress time t^{egress}. The travel times t^{ω}_{ri} (resp. t^{ω}_{js}) correspond to the shortest travel time between the origin r and the pick up i of our road network (resp. the drop off j and the destination s). At the end, we obtain the set of the potential pick ups $P^{\omega}_{r} = \{i \in P : t^{\omega}_{ri} \leq t^{\text{access}}\}$ among all the pick ups P and the set of potential drop offs $D^{\omega}_{s} = \{j \in D : t^{\omega}_{js} \leq t^{\text{egress}}\}$ among all the drop offs D. From these potential pick ups and drop offs, we extract for each OD pair the set $\Sigma^{\omega}_{rs} = \{(i, j) : i \in P^{\omega}_{r}, j \in D^{\omega}_{s}, (r, s) \in W^{\omega}\}$ of the P&R alternatives which corresponds to the possible combinations of pick ups and drop offs at each OD pair.

To determine the mode choice via a market share model based on a logit formulation, we use, for each itinerary, a generalized cost g^{ω}_{rijs} (resp. g^{ω}_{rmns}) composed of the travel cost between r and s using the proposed P&R system, that we consider equal to the travel time, between the three parts of the path: from the origin r to the pick up i (resp. m), $c^{\text{access},\omega}_{ri}$, from the pick up i (resp. m) to the drop off j (resp. n), $c^{\text{route},\omega}_{ij}$, and from the drop off j (resp. n) to the destination s, c^{walk}_{js}. When using the reserve mode to realize the entire itinerary, symbolized as R_{rs}, the travel cost $c^{\mathsf{R}_{rs},\omega}_{rs}$, equal to the generalized cost $g^{\mathsf{R}_{rs}}_{rs}$, is modeled as the travel time to reach the destination s from the origin r by car. We denote θ the logit parameter corresponding to the users' sensitivity to the generalized cost. The higher is θ, the more people are sensitive to the travel cost and will chose the cheaper transport mode. Finally, the parameters $-\theta g^{\mathsf{R}_{rs}}_{rs}$ correspond to the utility of the reserve mode and $-\theta g^{\omega}_{rijs}$ (resp. $-\theta g^{\omega}_{rmns}$) represent the utility of the P&R system from the pick up i (resp. m) to the drop off j (resp. n) for the path going from the origin r to the destination s. Although simple, our utility function considers the travel time preference in the mode choice. A more complex function could more accurately represent this mode choice, for instance by being trip purpose-dependent (Andrejszki et al., 2015).

A budget B is allowed to the construction of the pick ups and the drop offs whose costs $\boldsymbol{c}^{\text{loc}}_{i}$ mostly depends on the nature of the facility. Whereas car parks must be constructed at the pick ups locations for users to park their cars and embark the shuttles of the P&R system, transit stops are sufficient to leave the shuttle and reach the final destination by walk. We define a binary decision variable $y_i \in \{0, 1\}, \forall i \in P \cup D$, indicating the facility locations by being equal to one when a car park (pick up) or a transit stop (drop off) is open. Further, we define the decision variable $x^{\omega}_{rijs} \in \mathbb{R}^{+}, \quad \forall \omega \in \Omega, \forall (r, s) \in W^{\omega}, \forall (i, j) \in \Sigma^{\omega}_{rs} \cup \{\mathsf{R}_{rs}\}$, as the flow which determines the part of the scenario-dependent demand d^{ω}_{rs} associated to our P&R system on the OD pair (r, s) using the pick up i and the drop off j. The decision variable $x^{\omega,\mathsf{R}_{rs}}_{rs}$ defines the part of the users that choose the reserve mode on the OD pair (r, s).

All the mathematical notations are summarized in Table 1.

3.3. Mode choice model

The mode-choice behaviour and the route choice are emulated by means of a market share model based on a logit formulation, widely used in the field of transportation (Aros-Vera et al., 2013; Chen et al., 2016; Huang et al., 2018; Jian et al., 2019). The probability of choosing a transport mode for a specific itinerary is equal to the ratio of the exponential of the utility $e^{-\theta g^{\omega}_{rijs}}$ of this transport mode and the sum of the utilities for all the other transport mode. It is important to notice that in our model, each combination of pick up and drop off available to realize the itinerary is a possible choice for the transport mode. At the end, the transport mode alternatives are the reserve mode and the shuttle service of the proposed P&R from all accessible pick ups i to all accessible drop offs j.

Sets	**Definition**
Ω	Set of stochastic scenarios
N	Set of nodes in the network
E	Set of edges in the network
$W^\omega \subset N \times N$	Set of OD pairs in scenario $\omega \in \Omega$.
$P \subset N$	Set of pick up nodes.
$P_r^\omega \subset P$	Set of accessible pick ups nodes from the origin node $r \in N$ in scenario $\omega \in \Omega$.
$D \subset N$	Set of drop off nodes.
$D_s^\omega \subset D$	set of accessible drop offs nodes from the destination node $s \in N$ in scenario $\omega \in \Omega$.
$\Sigma_{rs}^\omega \subset N \times N$	Set of P&R paths in scenario $\omega \in \Omega$ for OD $(r,s) \in W^\omega$. Each element $(i,j) \in \Sigma_{rs}^\omega$ corresponds to the path (r,i,j,s) in the P&R system.
Parameters	
p^ω	Probability of the scenario $\omega \in \Omega$.
d_{rs}^ω	Travel demand in scenario $\omega \in \Omega$ for OD pair $(r,s) \in W^\omega$.
c_i^{loc}	Construction cost of a pick up (car park) or a drop off (transit stop) at node $i \in P \cup D$.
B	Budget available for the construction of pick up and drop off nodes
$c_{ri}^{\text{access},\omega}$	Travel time, assumed to be assess by car, allowing to reach the pick up i from the origin r
$c_{ij}^{\text{route},\omega}$	Travel time from pick up $i \in P$ to drop off $j \in D$ through the P&R system.
c_{js}^{walk}	Travel time from drop off $j \in D$ to destination $s \in N$ (assumed to be walking).
g_{rijs}^ω	Generalized cost of path (r,i,j,s) in the P&R system.
θ	Parameter in the logit model representing users' sensitivity to the generalized cost.
Decision variables	
$x_{rijs}^\omega \in [0,1]$	Proportion of users in scenario $w \in \Omega$ on OD $(r,s) \in W^\omega$ using the P&R system via path (r,i,j,s).
$x_{\mathsf{R}_{rs}}^\omega \in [0,1]$	Proportion of users using the reserve mode in scenario $w \in \Omega$ on OD $(r,s) \in W^\omega$.
$y_i \in \{0,1\}$	Decision to open a pick up or drop off facility at node $i \in P \cup D$.

Table 1
Notation table

As Aros-Vera et al. (2013) pointed out, we do not know which pick ups or drop offs are open before the solution of the model. For this reason, we adapt the logit formulation to consider all the transport mode alternative possibilities. Because both pick up and drop off have to be open to be considered as an option in the mode choice, the exponential of the utility for all the transport mode possibilities are multiplied by the pick up and the drop off location decision variables y_i and y_j. The closure of a pick up, a drop off or both will remove the consideration of the associated transport modes in the logit computation. For the sake of simplicity, in the implementation of the model, we consider $x_{rs}^{\omega,\mathsf{R}_{rs}}$ and x_{rijs}^ω as a unique variable where i and j could take the value R_{rs}, symbolizing the use of the reserve mode to realize the entire itinerary. At the end, the probability that users choose the pair i and j of the P&R system is:

$$x_{rijs}^\omega \equiv \frac{y_i y_j e^{-\theta g_{rijs}^\omega}}{\sum_{(m,n)\in\Sigma_{rs}^\omega \cup \{\mathsf{R}_{rs}\}} y_m y_n e^{-\theta g_{rmns}^\omega}} \quad \forall (r,s) \in W, \forall (i,j) \in \Sigma_{rs}^\omega \cup \{\mathsf{R}_{rs}\} \tag{1}$$

Variable x^{ω}_{rijs} represents the probability of using the reserve mode between the OD pair (r, s), when i and j are equal to R_{rs}, as well as the probability of using the proposed P&R system by using a shuttle joining the pick up i to the drop off j for the OD pair (r, s). The consideration of the possible use of a pick up and a drop off depends on the opening of both locations, *i.e.*, $y_i = 1$ *and* $y_j = 1$. If the pick up i or the drop off j or both are not located (*i.e.*, $y_i = 0$, $y_j = 0$ or $y_i = 0$ *and* $y_j = 0$) the probability of using this transport mode is null. The reserve mode, conversely, is always a possible alternative to perform a trip between an origin r and a destination s, as $y_{\mathsf{R}_{rs}}$ is always equal to one. It is worth to recall that θ symbolizes the users' sensitivity to the generalized costs $g^{\mathsf{R}_{rs}}_{rs}$, which corresponds to the travel time between r and s using the reserve mode and the parameter g^{ω}_{rijs} (resp. g^{ω}_{rmns}) corresponds to the travel time between r and s using the P&R system from the pick up i (resp. m) to the drop off j (resp. n) for the path going from the origin r to the destination s.

3.4. Flow and linking constraints

The linearization of the market share equation given by the logit model (1) is essential to consider the mode choice in our Mixed-Integer Linear Programming (MILP) problem. The combination of the following equations (2a), (2b), (2c) and (2d), based on the ones proposed by Aros-Vera et al. (2013), reproduce the logit formulation and represents the proportion of the users for each mobility alternative.

$$\sum_{(i,j)\in\Sigma^{\omega}_{rs}\cup\{\mathsf{R}_{rs}\}} x^{\omega}_{rijs} = 1 \qquad \forall\omega\in\Omega, \forall(r,s)\in W^{\omega} \tag{2a}$$

$$x^{\omega}_{rijs} \le x^{\omega}_{rmns}\frac{e^{-\theta g^{\omega}_{rijs}}}{e^{-\theta g^{\omega}_{rmns}}} + (2 - y_m - y_n) \qquad \forall\omega\in\Omega, \forall(r,s)\in W^{\omega}, \forall(m,n),(i,j)\in\Sigma^{\omega}_{rs}\cup\{\mathsf{R}_{rs}\} : \forall(m,n),(i,j)\in\Sigma^{\omega}_{rs}\cup\{\mathsf{R}_{rs}\} : (i,j)\neq(m,n) \tag{2b}$$

$$x^{\omega}_{rijs} \le y_i \qquad \forall\omega\in\Omega, \forall(r,s)\in W^{\omega}, \forall(i,j)\in\Sigma^{\omega}_{rs} \tag{2c}$$

$$x^{\omega}_{rijs} \le y_j \qquad \forall\omega\in\Omega, \forall(r,s)\in W^{\omega}, \forall(i,j)\in\Sigma^{\omega}_{rs} \tag{2d}$$

$$x^{\omega}_{rijs} \ge 0 \qquad \forall\omega\in\Omega, \forall(r,s)\in W^{\omega}, \forall(i,j)\in\Sigma^{\omega}_{rs}\cup\{\mathsf{R}_{rs}\} \tag{2e}$$

$$y_{\mathsf{R}_{rs}} = 1 \qquad \forall\omega\in\Omega, \forall(r,s)\in W^{\omega} \tag{2f}$$

$$y_i \in \{0,1\} \qquad \forall i\in P\cup D \tag{2g}$$

The first constraint (2a) ensures that the whole demand is served for each origin-destination pair. Users must perform these trips through the P&R system or using the reserve mode. The second constraint (2b) requires that the flow share of each mobility alternative obey to a logit model. For each OD pair, this choice is governed by the utility of mobility alternatives through the P&R system which is function of opened P&R facilities and of that of the reserve mode. For a given P&R path (r, i, j, s), if the pick up location y_i or the drop off location y_j or both are closed, the constraint is inactive due to linking constraints (2c) and (2d), forcing the flow share to be lower than one when parks are open, and zero otherwise. For a given OD pair (r, s), it is only possible to have a non zero portion of users use path (r, i, j, s) if and only if $y_i = y_j = 1$. The decision variable representing the portion of users going from the origin r to the destination s through the pick up i and the drop off j, x^{ω}_{rijs}, must be positive (2e). Constraints (2f) and (2g) set the domain of binary variables y_i and fix all such variables to one for the mobility alternative corresponding to the reserve mode.

The following result is an extension of the result of Aros-Vera et al. (2013) for three-link trip chains.

Proposition 1. *The set of integer-linear constraints* (2) *is equivalent to the logit formulation* (1).

Proof. The proof logic is based on the proof of Theorem 1 in Aros-Vera et al. (2013). To demonstrate the equivalence of both equations (1) and (2), we enumerate the four possible cases depending on facility location decisions at nodes i and j. For any scenario $\omega\in\Omega$ and for any OD pair $(r, s)\in W^{\omega}$:

- **At least one facility (pick up or drop off) is closed ($y_i = 0$ and $y_j = 1$; $y_i = 1$ and $y_j = 0$; or $y_i = y_j = 0$):**

If $y_i = 0$ or $y_j = 0$ for a pair $(i,j) \in \Sigma^{\omega}_{rs} \cup \{\mathsf{R}_{rs}\}$, from (1), it is immediate to see that $x^{\omega}_{rijs} = 0$. We show that (2) also yields the same outcome. In this case, the linking constraints (2c) or/and (2d) impose $x^{\omega}_{rijs} \leq 0$. Since the decision variable is required to be non-negative, i.e., $x^{\omega}_{rijs} \geq 0$, this implies $x^{\omega}_{rijs} = 0$. Furthermore, on the one hand, if $y_m = 0$ or (resp. and) $y_n = 0$ in constraint (2b), then the flow share on any concurrent mobility alternative $(i,j) \in \Sigma^{\omega}_{rs} \cup \{\mathsf{R}_{rs}\}$ is unrestricted. Indeed in such situation, $x^{\omega}_{rmns} = 0$ because of the linking constraints (2c) or (resp. and) (2d). If only one of the two parks is closed ($y_m = 0$ or $y_n = 0$), we obtain $x^{\omega}_{rijs} \leq 1$ which is already induced by the linking constraints (2c) and (2d); while if both parks are closed (y_m=0 and $y_n = 0$), $x^{\omega}_{rijs} \leq 2$ which is also redundant. On the other hand, if $y_m = y_n = 1$ in constraint (2b), then the flow share on any concurrent mobility alternative $(i,j) \in \Sigma^{\omega}_{rs} \cup \{\mathsf{R}_{rs}\}$ is upper-bounded by $x^{\omega}_{rmns} \frac{e^{-\theta g^{\omega}_{rijs}}}{e^{-\theta g^{\omega}_{rmns}}} \geq 0$ which is redundant since $x^{\omega}_{rijs} = 0$. This shows the equivalence of (1) and (2) if at least one facility is closed.

- **Both pick up and drop off are open ($y_i = y_j = 1$):**

If $y_i = y_j = 1$ for a pair $(i,j) \in \Sigma^{\omega}_{rs} \cup \{\mathsf{R}_{rs}\}$, from (1), we find that x^{ω}_{rijs} is equal to the flow share $x^{\omega}_{rmns} \frac{e^{-\theta g^{\omega}_{rijs}}}{\sum_{(m,n)\in\Sigma^{\omega}_{rs}\cup\{\mathsf{R}_{rs}\}:\, y_m=y_n=1} e^{-\theta g^{\omega}_{rmns}}}$, which corresponds to the flow share of alternative (i,j) in the presence of activated ($y_m = y_n = 1$) concurrent alternatives (m,n), as determined by a logit formulation. From (2), if $y_i = y_j = 1$, then the linking constraints (2c) and (2d) yield a unit upper bound on x^{ω}_{rijs} and constraint (2b) yield additional upper bounds for each activated ($y_m = y_n = 1$) concurrent alternative. Consider now a pair of activated alternatives (i,j) and (m,n). The corresponding pair of constraints (2b) require $x^{\omega}_{rijs} \leq x^{\omega}_{rmns} \frac{e^{-\theta g^{\omega}_{rijs}}}{e^{-\theta g^{\omega}_{rmns}}}$ and $x^{\omega}_{rmns} \leq x^{\omega}_{rijs} \frac{e^{-\theta g^{\omega}_{rmns}}}{e^{-\theta g^{\omega}_{rijs}}}$, implying $x^{\omega}_{rmns} = x^{\omega}_{rijs} \frac{e^{-\theta g^{\omega}_{rmns}}}{e^{-\theta g^{\omega}_{rijs}}}$. Assume that $|\Sigma^{\omega}_{rs}| = k$. From constraint (2a), we have:

$$x^{\omega,\mathsf{R}_{rs}}_{rs} + x^{\omega}_{ri_1j_1s} + \ldots + x^{\omega}_{rijs} + \ldots + x^{\omega}_{ri_kj_ks} = 1$$

$$\frac{e^{-\theta g^{\omega}_{\mathsf{R}_{rs}}}}{e^{-\theta g^{\omega}_{rijs}}} x^{\omega}_{rijs} + \frac{e^{-\theta g^{\omega}_{ri_1j_1s}}}{e^{-\theta g^{\omega}_{rijs}}} x^{\omega}_{rijs} + \ldots + \frac{e^{-\theta g^{\omega}_{rijs}}}{e^{-\theta g^{\omega}_{rijs}}} x^{\omega}_{rijs} + \ldots + \frac{e^{-\theta g^{\omega}_{ri_kj_ks}}}{e^{-\theta g^{\omega}_{rijs}}} x^{\omega}_{rijs} = 1$$

Re-arranging yields:

$$x^{\omega}_{rijs} = \frac{e^{-\theta g^{\omega}_{rijs}}}{\sum_{(m,n)\in\Sigma^{\omega}_{rs}\cup\{\mathsf{R}_{rs}\}} e^{-\theta g^{\omega}_{rmns}}}$$

which completes the proof of equivalence between Eqs. (1) and (2). □

3.5. Budget constraint and objective function

The P&R model aims at maximizing the part of users of the P&R system, by opening some facility locations, within a set of candidates, accessible from the users' origin and destination. The determination of the scenario-dependent flow per pick up/drop off path insights about the fleet sizing needed for a specific event. In the proposed P&R model, the facility location variable is binary due to the two potential state of the parks (closed or open) and is constrained by the park construction cost c^{loc}_i and the global allocated budget B.

$$\sum_{i\in P\cup D} c^{\text{loc}}_i y_i \leq B \tag{3}$$

The budget constraint (3) determines the ability of building the facilities by satisfying the global cost of the open parks. The objective function aims to maximize the expected ridership in the P&R system across stochastic scenarios and can be written as:

$$\max \quad \sum_{\omega\in\Omega} p^{\omega} \sum_{(r,s)\in W^{\omega}} d^{\omega}_{rs} \sum_{(i,j)\in\Sigma^{\omega}_{rs}} x^{\omega}_{rijs} \tag{4}$$

By maximizing the objective function (4), the solution increases for all the OD pairs (r, s) the portion x^{ω}_{rijs} of the demand d^{ω}_{rs} using our P&R system whatever the chosen pick up i and drop off j in each scenario ω. The higher the probability p^{ω} related to the occurrence of an event is, the more the system will fit it. By being attractive in terms of travel time with the car parks and transit stops opening, the P&R system helps to reduce the private vehicle circulation in the city center of the cities and increase its resilience with respect to recurrent disruptive scenarios by providing an alternative transport mode.

3.6. Park and ride facility location formulation

The resulting P&R facility location formulation summarized in (5) is a MILP. The complexity of the problem highly increases with the graph size due to the number of variables, as detailed in Section 6.1.1: for the small network composed of 59 nodes used in our numerical experiments, the formulation corresponds to 267 000 constraints and 15 000 variables; the problem grows to 15 000 000 constraints and 270 000 variables for the larger one, composed of 135 nodes. We thus propose, in the next Section 4, a scalable approach that can accommodate large mobility networks.

$$\max \quad \sum_{\omega\in\Omega} p^{\omega} \sum_{(r,s)\in W^{\omega}} d^{\omega}_{rs} \sum_{(i,j)\in\Sigma^{\omega}_{rs}} x^{\omega}_{rijs} \tag{5a}$$

$$\text{s.t.} \sum_{i\in P\cup D} c^{\text{loc}}_{i} y_i \leq B \tag{5b}$$

$$\sum_{(i,j)\in\Sigma^{\omega}_{rs}\cup\{\mathsf{R}_{rs}\}} x^{\omega}_{rijs} = 1 \qquad \forall\omega\in\Omega, \forall(r,s)\in W^{\omega} \tag{5c}$$

$$x^{\omega}_{rijs} \leq x^{\omega}_{rmns} \frac{e^{-\theta g^{\omega}_{rijs}}}{e^{-\theta g^{\omega}_{rmns}}} + (2 - y_m - y_n) \qquad \forall\omega\in\Omega, \forall(r,s)\in W^{\omega}, \forall(m,n),(i,j)\in\Sigma^{\omega}_{rs}\cup\{\mathsf{R}_{rs}\} : (i,j)\neq(m,n) \tag{5d}$$

$$x^{\omega}_{rijs} \leq y_i \qquad \forall\omega\in\Omega, \forall(r,s)\in W^{\omega}, \forall(i,j)\in\Sigma^{\omega}_{rs} \tag{5e}$$

$$x^{\omega}_{rijs} \leq y_j \qquad \forall\omega\in\Omega, \forall(r,s)\in W^{\omega}, \forall(i,j)\in\Sigma^{\omega}_{rs} \tag{5f}$$

$$y_{\mathsf{R}_{rs}} = 1 \qquad \forall\omega\in\Omega, \forall(r,s)\in W^{\omega} \tag{5g}$$

$$x^{\omega}_{rijs} \geq 0 \qquad \forall\omega\in\Omega, \forall(r,s)\in W^{\omega}, \forall(i,j)\in\Sigma^{\omega}_{rs} \tag{5h}$$

$$y_i \in \{0,1\} \qquad \forall i\in P\cup D \tag{5i}$$

4. Lagrangian relaxation algorithm

To efficiently solve the proposed P&R facility location problem represented by Formulation (5), we adopt a decomposition approach based on Lagrangian Relaxation (LR). The proposed LR provides upper bounds on the original problem and we present customized heuristic algorithms to iteratively generate lower bounds during the solution of the LR problem. We first present the proposed LR formulations and introduce a subgradient algorithm to solve the LR problem (Section 4.1) before discussing the heuristic algorithms to generate feasible solutions (Section 4.2).

4.1. Lagrangian relaxation formulations

Let $\boldsymbol{x}$ be the vector of scenario-based flow variables x^{ω}_{rijs} and let $\boldsymbol{y}$ be the vector of facility location variables y_i. We dualize constraints (5d), (5e) and (5f) which contain both flow variables (x_{rijs}) and location variables (y_i). Let $\lambda^{\omega}_{rijmns} \geq 0$ be Lagrange multipliers (LM) for constraint (5d) (with matching indices); let $\pi^{\omega}_{rijs} \geq 0$ be LM for constraint (5e); and let $\delta^{\omega}_{rijs} \geq 0$ be LM for constraint (5f). Let $L(\boldsymbol{\pi}, \boldsymbol{\delta}, \boldsymbol{\lambda})$ be the Lagrangian function, the resulting Lagrangian relaxation of (5) is summarized in Formulation (6). The LR formulation (6) provides an upper bound on the objective value of Formulation (5).

$$L(\boldsymbol{\pi}, \boldsymbol{\delta}, \boldsymbol{\lambda}) = \max \quad \sum_{\omega\in\Omega} p^{\omega} \sum_{(r,s)\in W^{\omega}} d^{\omega}_{rs} \sum_{(i,j)\in\Sigma^{\omega}_{rs}} x^{\omega}_{rijs}$$

$$+ \sum_{\omega\in\Omega} \sum_{(r,s)\in W^\omega} \sum_{(i,j)\in\Sigma^\omega_{rs}} \left(\pi^\omega_{rijs}(y_i - x^\omega_{rijs}) + \delta^\omega_{rijs}(y_j - x^\omega_{rijs})\right)$$

$$+ \sum_{\omega\in\Omega} \sum_{(r,s)\in W^\omega} \sum_{(i,j)\in\Sigma^\omega_{rs}\cup\{\mathsf{R}_{rs}\}} \sum_{\substack{(m,n)\in\Sigma^\omega_{rs}\cup\{\mathsf{R}_{rs}\},\\ (m,n)\neq(i,j)}} \lambda^\omega_{rijmns}\left(x^\omega_{rmns}\frac{e^{-\theta g^\omega_{rijs}}}{e^{-\theta g^\omega_{rmns}}} + 2 - y_m - y_n - x^\omega_{rijs}\right) \tag{6a}$$

$$\text{s.t.} \sum_{i\in P\cup D} c^{\text{loc}}_i y_i \leq B \tag{6b}$$

$$\sum_{(i,j)\in\Sigma^\omega_{rs}\cup\{\mathsf{R}_{rs}\}} x^\omega_{rijs} = 1 \qquad \forall\omega\in\Omega, \forall(r,s)\in W^\omega \tag{6c}$$

$$x^\omega_{rijs} \geq 0 \qquad \forall\omega\in\Omega, \forall(r,s)\in W^\omega, \forall(i,j)\in\Sigma^\omega_{rs}\cup\{\mathsf{R}_{rs}\} \tag{6d}$$

$$y_{\mathsf{R}_{rs}} = 1 \qquad \forall\omega\in\Omega, \forall(r,s)\in W^\omega \tag{6e}$$

$$y_i \in \{0,1\} \qquad \forall i\in P\cup D \tag{6f}$$

The motivation for this LR formulation is that by relaxing the constraints involving both variables $\boldsymbol{x}$ and $\boldsymbol{y}$, *i.e.*, (5e), (5f) and (5d), the resulting formulation (6) can be separated into two sub-problems: i) a linear assignment problem in $\boldsymbol{x}$ to distribute users within paths of the P&R system or their reserve mode (7); and, ii) a facility location problem in $\boldsymbol{y}$ which is an integer-linear problem (8) that is expected to be easier to solve than Formulation (5). Let $L_{\boldsymbol{x}}(\boldsymbol{\pi},\boldsymbol{\delta},\boldsymbol{\lambda})$ be the part of $L(\boldsymbol{\pi},\boldsymbol{\delta},\boldsymbol{\lambda})$ which contains exclusively terms in $\boldsymbol{x}$; and let $L_{\boldsymbol{y}}(\boldsymbol{\pi},\boldsymbol{\delta},\boldsymbol{\lambda})$ be the part of $L(\boldsymbol{\pi},\boldsymbol{\delta},\boldsymbol{\lambda})$ which contains exclusively terms in $\boldsymbol{y}$. The Lagrangian sub-problem corresponding to variable $\boldsymbol{x}$ is summarized in Formulation (7).

$$L_{\boldsymbol{x}}(\boldsymbol{\pi},\boldsymbol{\delta},\boldsymbol{\lambda}) = \max \sum_{\omega\in\Omega} p^\omega \sum_{(r,s)\in W^\omega} d^\omega_{rs} \sum_{(i,j)\in\Sigma^\omega_{rs}} x^\omega_{rijs} - \sum_{\omega\in\Omega} \sum_{(r,s)\in W^\omega} \sum_{(i,j)\in\Sigma^\omega_{rs}} \left(\pi^\omega_{rijs} + \delta^\omega_{rijs}\right) x^\omega_{rijs}$$

$$+ \sum_{\omega\in\Omega} \sum_{(r,s)\in W^\omega} \sum_{(i,j)\in\Sigma^\omega_{rs}\cup\{\mathsf{R}_{rs}\}} \sum_{\substack{(m,n)\in\Sigma^\omega_{rs}\cup\{\mathsf{R}_{rs}\},\\ (m,n)\neq(i,j)}} \lambda^\omega_{rijmns}\left(x^\omega_{rmns}\frac{e^{-\theta g^\omega_{rijs}}}{e^{-\theta g^\omega_{rmns}}} - x^\omega_{rijs}\right) \tag{7a}$$

$$\text{s.t.} \sum_{(i,j)\in\Sigma^\omega_{rs}\cup\{\mathsf{R}_{rs}\}} x^\omega_{rijs} = 1 \qquad \forall\omega\in\Omega, \forall(r,s)\in W^\omega \tag{7b}$$

$$x^\omega_{rijs} \geq 0 \qquad \forall\omega\in\Omega, \forall(r,s)\in W^\omega, \forall(i,j)\in\Sigma^\omega_{rs}\cup\{\mathsf{R}_{rs}\} \tag{7c}$$

$L_{\boldsymbol{x}}$ can be further decomposed into scenario-based sub-problems by separating flows variables $\boldsymbol{x}$ corresponding to each scenario $\omega\in\Omega$. Hence, we denote $L_{\boldsymbol{x},\omega}$ the Lagrangian sub-problem of $L_{\boldsymbol{x}}$ for scenario $\omega\in\Omega$ and the following relationship holds: $L_{\boldsymbol{x}}(\boldsymbol{\pi},\boldsymbol{\delta},\boldsymbol{\lambda}) = \sum_{\omega\in\Omega} L_{\boldsymbol{x},\omega}(\boldsymbol{\pi},\boldsymbol{\delta},\boldsymbol{\lambda})$.

The Lagrangian sub-problem corresponding to variable $\boldsymbol{y}$ is summarized in Formulation (8).

$$L_{\boldsymbol{y}}(\boldsymbol{\pi},\boldsymbol{\delta},\boldsymbol{\lambda}) = \max \sum_{\omega\in\Omega} \sum_{(r,s)\in W^\omega} \sum_{(i,j)\in\Sigma^\omega_{rs}} \left(\pi^\omega_{rijs} y_i + \delta^\omega_{rijs} y_j\right)$$

$$+ \sum_{\omega\in\Omega} \sum_{(r,s)\in W^\omega} \sum_{(i,j)\in\Sigma^\omega_{rs}\cup\{\mathsf{R}_{rs}\}} \sum_{\substack{(m,n)\in\Sigma^\omega_{rs}\cup\{\mathsf{R}_{rs}\},\\ (m,n)\neq(i,j)}} \lambda^\omega_{rijmns}(2 - y_m - y_n) \tag{8a}$$

$$\text{s.t.} \sum_{i\in P\cup D} c^{\text{loc}}_i y_i \leq B \tag{8b}$$

$$y_{\mathsf{R}_{rs}} = 1 \qquad \forall\omega\in\Omega, \forall(r,s)\in W^\omega \tag{8c}$$

$$y_i \in \{0,1\} \qquad \forall i \in P \cup D \tag{8d}$$

For any vector of LM $\boldsymbol{\pi}$, $\boldsymbol{\delta}$ and λ, $L(\boldsymbol{\pi},\boldsymbol{\delta},\lambda) = L_{\boldsymbol{x}}(\boldsymbol{\pi},\boldsymbol{\delta},\lambda) + L_{\boldsymbol{y}}(\boldsymbol{\pi},\boldsymbol{\delta},\lambda)$. Observe that Formulation (7) is a linear programming problem and that Formulation (8) is binary knapsack problem. Both of these formulations are expected to be significantly easier to solve than the MILP formulation (5).

4.2. Solution algorithm

The Lagrangian subgradient algorithm provides a method to explore the solution space of the P&R facility location problem but only generates relaxed solutions at each iteration. An overview of the LRA is detailed in Algorithm 1. The goal of LR is to find the LM $\boldsymbol{\pi}^\star$, $\boldsymbol{\delta}^\star$ and $\lambda^\star$ which maximize $L(\boldsymbol{\pi},\boldsymbol{\delta},\lambda)$ so that the lower bound is as tight as possible (ideally equal) to the optimal objective value. To solve the LR problem, we use the traditional subgradient algorithm. Such choice is motivated by the easy computation of the method and its ability to properly solve several practical problems (Fischer et al., 2013).

The proposed LRA is presented in Algorithm 1. As a first step of the LRA, we initialize the LMs and the iteration counter. A first lower bound LB^0, issued from the constructed vectors $\hat{\boldsymbol{x}}^0$ and $\hat{\boldsymbol{y}}^0$, is computed using the heuristic described in Algorithm 2, before beginning the iterations. Such step could help the proposed LRA to converge if this LB^0 is better than the lower bound issued from the iterations, especially when the problem complexity limits the number of iterations in a given time. Although simplistic, the heuristic provides more accurate results, with a higher lower bound and a lower gap between the lower and the upper bounds, for large-scale instances than the one obtained in a very small set of iterations of the proposed LA. In this heuristic we first open all the locations y_i to compute the feasible flow x^{ω}_{rijs} (Alg. 3), with the market share model issued from the logit formula (1), for each scenario, each origin/destination pair and each pick up/drop off or reserve mode of the P&R model, in order to know the flow crossing each location. After sorting the decision variable y_i, depending on the ratio of the construction cost over the part of the flow of users crossing each facility, then we close the car park and/or transit stop with the higher ratio, while the budget constraint is respected. The new corresponding flow is computed using the logit formulation (Alg. 3). As a final step, the lower bound is computed, issued from the objective function. The combination of this heuristic (Alg. 2) with the LRA ensures a reduced gap between the lower and the upper bounds especially for large scale instance.

After initializing the parameters and computing a first lower bound, we begin the LR (Alg. 1, line 1 to line 5). At each iteration n we repeat the same steps. First, we compute the optimal solution for of sub-problems $L_{\boldsymbol{x}}(\boldsymbol{\pi},\boldsymbol{\delta},\lambda)$ and $L_{\boldsymbol{y}}(\boldsymbol{\pi},\boldsymbol{\delta},\lambda)$. The first sub-problem $L_{\boldsymbol{x}}(\boldsymbol{\pi},\boldsymbol{\delta},\lambda)$ provides a vector $\boldsymbol{x}^n$ (Alg. 1, line 8 to line 11) which may not be feasible. To obtain a feasible solution from this vector, we build a feasible vector $\hat{\boldsymbol{y}}^n$ from $\boldsymbol{x}^n$ (Alg. 1, line 12). To that purpose, we open all the parks crossed by a non zero flow. If opening all these parks violates the budget constraint, we close the pick up and/or drop off whose ratio of construction cost over the crossing flow is the highest, until the budget constraint is satisfied. Finally, we recompute the flow $\boldsymbol{x}'^n$ corresponding to the P&R design $\hat{\boldsymbol{y}}^n$ (Alg. 4).

The second sub-problem $L_{\boldsymbol{y}}(\boldsymbol{\pi},\boldsymbol{\delta},\lambda)$ gives a solution $\boldsymbol{y}^n$ (Alg. 1, line 13). We use the logit formula to obtain a feasible flow pattern $\hat{\boldsymbol{x}}^n$ corresponding to this P&R design solution (Alg. 5) (Alg. 1, line 14). Once the two feasible solutions are established $(\boldsymbol{x}^n, \hat{\boldsymbol{y}}^n)$ and $(\hat{\boldsymbol{x}}^n, \boldsymbol{y}^n)$ we are able to compute both corresponding lower bounds $\mathsf{LB}^n_{L_x}$ and $\mathsf{LB}^n_{L_y}$ respectively issued from $L_{\boldsymbol{x}}(\boldsymbol{\pi},\boldsymbol{\delta},\lambda)$ and $L_{\boldsymbol{y}}(\boldsymbol{\pi},\boldsymbol{\delta},\lambda)$. The higher of the two is conserved as a local lower bound LB^n and the couple of vectors $(\boldsymbol{x}^{*,n}, \boldsymbol{y}^{*,n})$ corresponding to the best vectors combination, maximizing the lower bound, $(\boldsymbol{x}^n, \hat{\boldsymbol{y}}^n)$ or $(\hat{\boldsymbol{x}}^n, \boldsymbol{y}^n)$ is defined (Alg. 1, line 15 to line 19). The global lower bound LB, which corresponds to the highest lower bound obtained since the beginning of the LRA, including the first lower bound LB^0, is updated, as well as the couple of vectors $(\boldsymbol{x}, \boldsymbol{y})$, if and only if the local lower bound LB^n exceeds the global one.

To improve the performance of our heuristic, we apply local search algorithms for the solutions with the aim to further increase the previously discussed lower bound. To this purpose, we alternate between a neighbourhood search and swap moves until there is no improvement in the lower bound or all the local combinations have been explored. We also use a time limit constraint to avoid spending excessive computation time in the search procedure for local improvement of a given iteration of the LR (Alg. 1, line 21 to line 24). In our neighborhood exploration (Alg. 6), we sequentially set binary facility variables of the current best solution $\hat{\boldsymbol{y}}^n$ to their complementary value, *i.e.*, open parks that are closed and close parks that are open, provided that the budget constraint remains satisfied. For each solution in the neighborhood of the current best solution, we recalculate the flow assignment $\boldsymbol{x}$ (Alg. 3) and determine the corresponding objective value which will replace the local lower bound LB^n if the result is higher. The global lower bound LB should also be replaced by this solution if LB is lower.

Algorithm 1: Lagrangian Relaxation Algorithm Overview

Input: ϵ, TL^{glob}, TL^{heur}
Output: LB, UB, $\boldsymbol{x}$, $\boldsymbol{y}$
/* Initialization of bounds, LM and parameters */
1 $\mathsf{Gap} \leftarrow +\infty$
2 $\mathsf{UB} \leftarrow +\infty$
3 $\mathsf{LB} \leftarrow$ Algorithm 2 // Construct initial feasible solution
4 $\boldsymbol{\pi}, \boldsymbol{\delta}, \boldsymbol{\lambda} \leftarrow \mathbf{0}$
5 $\mathsf{TL}^{glob} \leftarrow 0$
6 $n \leftarrow 0$
/* Main loop */
7 **while** $\mathsf{Gap} > \epsilon$ ***or*** $\mathsf{Timer}^{glob} \leq \mathsf{TL}^{glob}$ **do**
8 **for** $\omega \in \Omega$ **do**
9 $\boldsymbol{x}^{\omega,n} \leftarrow$ Solve $L_{\boldsymbol{x},\omega}(\boldsymbol{\pi}, \boldsymbol{\delta}, \boldsymbol{\lambda})$
10 $L_{\boldsymbol{x}}(\boldsymbol{\pi}, \boldsymbol{\delta}, \boldsymbol{\lambda}) \leftarrow \sum_{\omega \in \Omega} L_{\boldsymbol{x},\omega}(\boldsymbol{\pi}, \boldsymbol{\delta}, \boldsymbol{\lambda})$
11 $\boldsymbol{x}^n \leftarrow [\boldsymbol{x}^{\omega,n}]_{\omega \in \Omega}$
12 $\hat{\boldsymbol{y}}^n, \boldsymbol{x}'^n, \mathsf{LB}^n_{L_x} \leftarrow$Algorithm 4 $(\boldsymbol{x}^n)$ // Construct feasible solution from $\boldsymbol{x}$
13 $\boldsymbol{y}^n \leftarrow$ Solve $L_{\boldsymbol{y}}(\boldsymbol{\pi}, \boldsymbol{\delta}, \boldsymbol{\lambda})$
14 $\hat{\boldsymbol{x}}^n, \mathsf{LB}^n_{L_y} \leftarrow$Algorithm 5 $(\boldsymbol{y}^n)$ // Construct feasible solution from $\boldsymbol{y}$
15 $\mathsf{LB}^n \leftarrow \max\{\mathsf{LB}^n_{L_x}, \mathsf{LB}^n_{L_y}\}$
16 **if** $\mathsf{LB}^n_{L_x} \geq \mathsf{LB}^n_{L_y}$ **then**
17 $(\boldsymbol{x}^{*,n}, \boldsymbol{y}^{*,n}) \leftarrow (\boldsymbol{x}'^n, \hat{\boldsymbol{y}}^n)$
18 **else**
19 $(\boldsymbol{x}^{*,n}, \boldsymbol{y}^{*,n}) \leftarrow (\hat{\boldsymbol{x}}^n, \boldsymbol{y}^n)$
20 $\mathsf{TL}^{heur} \leftarrow 0$
/* Local search loop */
21 **while** LB^n *improved by the local search* ***and*** $\mathsf{Timer}^{heur} \leq \mathsf{TL}^{heur}$ **do**
22 $\mathsf{LB}^n, \boldsymbol{x}^{*,n}, \boldsymbol{y}^{*,n} \leftarrow$ Algorithm 6 $(\mathsf{LB}^n, \boldsymbol{y}^{*,n})$ // 1-distance local search on $\boldsymbol{y}$
23 $\mathsf{LB}^n, \boldsymbol{x}^{*,n}, \boldsymbol{y}^{*,n} \leftarrow$ Algorithm 7 $(\mathsf{LB}^n, \boldsymbol{y}^{*,n})$ // Swap local search on $\boldsymbol{y}$
24 Update Timer^{heur}
25 **if** $\mathsf{LB}^n \geq \mathsf{LB}$ **then**
26 $\mathsf{LB} \leftarrow \mathsf{LB}^n$ $(\boldsymbol{x}, \boldsymbol{y}) \leftarrow (\boldsymbol{x}^{*,n}, \boldsymbol{y}^{*,n})$
27 $\mathsf{UB} \leftarrow \min\{\mathsf{UB}, L_{\boldsymbol{x}}(\boldsymbol{\pi}, \boldsymbol{\delta}, \boldsymbol{\lambda}) + L_{\boldsymbol{y}}(\boldsymbol{\pi}, \boldsymbol{\delta}, \boldsymbol{\lambda})\}$
28 $\mathsf{Gap} \leftarrow \frac{\mathsf{UB}-\mathsf{LB}}{\mathsf{UB}}$
29 Update LM using Eq. (9)
30 Update Timer^{glob}

We apply a second local search which swaps pairs of open and closed parks (Alg. 7). Contrary to the neighborhood local search, the $\boldsymbol{y}$ vector is modified in a way that a park opening is combined with a park closure and a park closure is paired with a park opening based on the respective park construction costs. We also recalculate the flow assignment $\boldsymbol{x}$ and modify the LB^n if the solution improves.

LM are updated at the end of each iteration of the main while loop using (9) (Alg. 1, line 29). To update the LM, we use a classical formulation (Fisher, 2004). If the constraints (2b), (2c) or (2d) are not respected, the corresponding LM $\lambda^{\omega}_{rijmns}$, π^{ω}_{rijs} or δ^{ω}_{rijs} are updated and become greater than 0. Indeed, if a flow share x^{ω}_{rijs} crosses a closed park y_i, $i \in P$ (resp. y_j, $j \in D$), the LM π^{ω}_{rijs} (resp. δ^{ω}_{rijs}) will increase to incentivize the constraint to be respected in the next iterations. Regarding $\lambda^{\omega}_{rijmns}$, the LM increases if the flow share does not follow the used market share model represented by the logit formula. Because we aim at maximizing the ridership, and because the LM are deducted from

Algorithm 2: First LB computation

Input:
Output: $\boldsymbol{x}^0$, $\boldsymbol{y}^0$, LB^0
for $i \in P \cup D$ **do**
  $\hat{y}_i^0 \leftarrow 1$ $f_i \leftarrow$ Sum of the flows $\boldsymbol{x}^0$ crossing i
$S_{\hat{y}^0} \leftarrow$ Sort $\hat{\boldsymbol{y}}^0$ increasingly by $\boldsymbol{c}_i^{\text{loc}}/f_i$
for $i \in S_{\hat{y}^0}$ **do**
  while $\sum_{j \in P \cup D} \boldsymbol{c}_j^{loc} y_j \geq B$ **do**
    $\hat{y}_i^0 \leftarrow 0$
$\hat{\boldsymbol{x}}^0 \leftarrow$ Feasible flow for the park design $\hat{\boldsymbol{y}}^0$ according to Eq. (1) using Algorithm 3
$\mathsf{LB}^0 \leftarrow$ Compute objective function (5a) for $(\hat{\boldsymbol{x}^0}, \hat{\boldsymbol{y}}^0)$ **while** LB^0 *improved by the local search* ***and*** $\mathsf{Timer}^{heur} \leq \mathsf{TL}^{heur}$ **do**
  $\mathsf{LB}^0, \hat{\boldsymbol{x}^0}, \hat{\boldsymbol{y}^0} \leftarrow$ Algorithm 6 $(\mathsf{LB}^0, \hat{\boldsymbol{y}^0})$ `// 1-distance local search on y`
  $\mathsf{LB}^0, \hat{\boldsymbol{x}^0}, \leftarrow$ Algorithm 7 $(\mathsf{LB}^0, \hat{\boldsymbol{y}^0})$ `// Swap local search on y`
  Update Timer^{heur}

Algorithm 3: Feasible flow computation

Input: $\boldsymbol{x}$
Output: $\boldsymbol{y}$
for $\omega \in \Omega$ **do**
  for $(r,s) \in W^\omega$ **do**
    for $(i,j) \in \Sigma_{rs}^\omega$ **do**
      $x_{rijs}^\omega \leftarrow \frac{y_i y_j e^{-\theta g_{rijs}^\omega}}{\sum_{(m,n) \in \Sigma_{rs}^\omega \cup \{\mathsf{R_{rs}}\}} y_m y_n e^{-\theta g_{rmns}^\omega}}$

the objective function, such updates will incentivize the constraints to be respected.

$$\pi_{rijs}^{\omega,n+1} = max\left(\pi_{rijs}^{\omega,n} + \gamma^n\left(x_{rijs}^{\omega,n} - y_i^n\right), 0\right) \qquad \forall \omega \in \Omega, \forall (r,s) \in W^\omega, \forall (i,j) \in \Sigma_{rs}^\omega \tag{9a}$$

$$\delta_{rijs}^{\omega,n+1} = max\left(\delta_{rijs}^{\omega,n} + \gamma^n\left(x_{rijs}^{\omega,n} - y_j^n\right), 0\right) \qquad \forall \omega \in \Omega, \forall (r,s) \in W^\omega, \forall (i,j) \in \Sigma_{rs}^\omega \tag{9b}$$

$$\lambda_{rijmns}^{\omega,n+1} = max\left(\lambda_{rijmns}^{\omega,n} + \gamma^n\left(x_{rmns}^{\omega}\frac{e^{-\theta g_{rijs}^\omega}}{e^{-\theta g_{rmns}^\omega}} + 2 - y_m - y_n - x_{rijs}^\omega\right), 0\right) \qquad \forall \omega \in \Omega, \forall (r,s) \in W^\omega, \forall (i,j) \in \Sigma_{rs}^\omega, \forall (m,n) \in \Sigma_{rs}^\omega : (i,j) \neq (m,n) \tag{9c}$$

To compute the step-size γ^n, we use the traditional formulation Fisher (2004); Lag.

$$\gamma^n = \alpha^n \frac{L(\boldsymbol{\pi}, \boldsymbol{\delta}, \boldsymbol{\lambda}) - \mathsf{LB}}{\left\|x_{rijs}^{\omega,n} - y_i^n\right\|_2 + \left\|x_{rijs}^{\omega,n} - y_j^n\right\|_2 + \left\|x_{rijs}^{\omega,n} - x_{rmns}^{\omega,n}\frac{e^{-\theta g_{rijs}^\omega}}{e^{-\theta g_{rmns}^\omega}} - 1 + y_{mn}^n\right\|_2} \tag{10a}$$

Algorithm 4: Construction of a feasible solution from L_x

Input: x^n
Output: $\hat{y}^n$, x'^n, $\mathsf{LB}^n_{L_x}$

for $(i,j) \in \Sigma^\omega_{rs}$ **do**
  if $x^\omega_{rijs} \neq 0$ **then**
    $(\hat{y}_i{}^n, \hat{y}_j{}^n) \leftarrow (1,1)$
$f_i \leftarrow$ Sum of the flows x^n crossing i
$S_{\hat{y}^n} \leftarrow$ Sort y by increasing c^{loc}_i / f_i
for $i \in S_{\hat{y}^n}$ **do**
  while $\sum_{j \in P \cup D} c^{loc}_j y_j \geq B$ **do**
    $\hat{y}^n_i \leftarrow 0$
$x'^n \leftarrow$ Feasible flow for the park design $\hat{y}^n$ (1)
$\mathsf{LB}^n_{L_x} \leftarrow$ Compute the objective function for $(x^n, \hat{y}^n)$ (5a) Algorithm 3

Algorithm 5: Construction of a feasible solution from L_y

Input: y^n
Output: $\hat{x}^n$, $\mathsf{LB}^n_{L_y}$

$\hat{x}^n \leftarrow$ Feasible flow for the park design y^n using the logit formula Eq. (1) Algorithm 3
$\mathsf{LB}^n_{L_y} \leftarrow$ Compute the objective function for $(\hat{x^n}, y^n)$ (5a)

$$\left\| x^{\omega,n}_{rijs} - y^n_i \right\|_2 = \sum_{\omega \in \Omega} \sum_{(r,s) \in W^\omega} \sum_{(i,j) \in \Sigma^\omega_{rs}} \left(x^{\omega,n}_{rijs} - y^n_i \right)^2 \tag{10b}$$

$$\left\| x^{\omega,n}_{rijs} - y^n_j \right\|_2 = \sum_{\omega \in \Omega} \sum_{(r,s) \in W^\omega} \sum_{(i,j) \in \Sigma^\omega_{rs}} \left(x^{\omega,n}_{rijs} - y^n_j \right)^2 \tag{10c}$$

$$\left\| x^{\omega,n}_{rijs} - x^{\omega,n}_{rmns} \frac{e^{-\theta g^\omega_{rijs}}}{e^{-\theta g^\omega_{rmns}}} - 1 + y^n_{mn} \right\|_2 = \sum_{(r,s) \in W^\omega} \sum_{(i,j) \in \Sigma^\omega_{rs}} \sum_{(m,n) \in \Sigma^\omega_{rs}} \left(x^{\omega,n}_{rijs} - x^{\omega,n}_{rmns} \frac{e^{-\theta g^\omega_{rijs}}}{e^{-\theta g^\omega_{rmns}}} - 1 + y^n_{mn} \right)^2 \tag{10d}$$

5. Case study

In this section, we present the data used to test the proposed methods. We first present the dataset (Sec. 5.1), then we introduce the P&R instances generated for the numerical experiments (Sec. 5.2).

5.1. Data preparation

For our case study, we use the road network of Lyon, France, composed of 10 905 nodes and 19 703 edges. The geography of the city constructed around a peninsula makes the center sensitive to disturbances due to the relatively weak number of alternative paths. The city center is also the location where most events take place and where businesses are attracting most people. Finally, the pedestrianisation of Lyon's peninsula is currently an active topic of discussion in the city[1]. For these reasons, we investigate the potential of an alternative, on-demand transport mode to improve accessibility and reduce the use of private vehicles. We focus on trips from outside the peninsula to the peninsula. All the destinations, which could be potential drop offs (j), are located in the 1^{st} and the 2^{nd} neighborhoods of Lyon which form the peninsula, whereas all the origins and potential pick ups (i) are sited in the rest of the city.

Travel times and travel costs are determined using floating car data (FCD) recorded by BeMobile operator[2] from

[1] https://www.lyoncapitale.fr/politique/pietonnisation-presqu-ile-a-lyon-la-coalition-climat-veut-des-actes/
[2] http://be-mobile.com

Algorithm 6: One distance neighborhood search

Input: LB^n, $\boldsymbol{y}^{*,n}$
Output: LB^n, $\boldsymbol{x}^{*,n}$, $\boldsymbol{y}^{*,n}$, $\boldsymbol{x}$, $\boldsymbol{y}$

```
update ← True
while update = True do
    update ← False
    for i ∈ P ∪ D do
        ȳ ← y^{*,n}
        if y_i^{*,n} = 1 then
            ȳ_i ← 0
        else
            ȳ_i ← 1
        x̄ ← Feasible flow for the park design ȳ (1) Algorithm 3
        LB̄ ← Compute the objective function for (x̄, ȳ) (5a)
        if LB̄ ≥ LB^n then
            LB^n ← LB̄
            (x^{*,n}, y^{*,n}) ← (x̄, ȳ)
            update ← True
            break
```

October 2017 to September 2018. This provides the travel cost, equal to the recorded travel time, for the proposed P&R system between the origin and the pick up $c_{ri}^{\text{access},\omega}$ and between the pick up and the drop off $c_{ij}^{\text{route},\omega}$. The travel cost between the drop off and the destination c_{js}^{walk} corresponds to the walking travel time and is computed through the road network using a walking speed of $1.5m/s$. The travel cost between the origin and the destination using the reserve mode $c_{rs}^{\mathsf{R}_{rs},\omega}$ corresponds to the travel time of the shortest path between the origin and the destination, recorded through the FCD. We do not consider the additional costs associated to the reserve transport mode (*e.g.*, fuel, parking, congestion, pollution) in accordance with the simplistic representation but the generalized cost computation could be improved in the future in accordance with the existing literature (Aros-Vera et al., 2013; Hitge and Vanderschuren, 2015).

During the recorded period, many events of different nature perturbing traffic conditions occurred such as snowfall, strike, road works or public transport disruptions, corresponding to recurrent disturbances. By selecting the recurrent abnormal traffic conditions in the FCD, as well as the baseline one, we build a first instance with four stochastic scenarios. These four scenarios have their own travel cost, recorded during different days whereas the construction cost is defined once and for all. To create other instances, used for the sensitivity analysis (Sec. 6.1), we only select different days recorded during the holidays, during the weekend and during the working days. In the sensitivity analysis (Sec. 6.1), the four scenarios have an equiprobability of happening.

For the realistic analysis (Sec. 6.2), the scenarios are recorded: *i)* during a snowfall, *ii)* with a public transport disruption where two subway lines were stopped, *iii)* during a normal week day, and *iv)* during a normal week end day. Each scenario presents a different speed profile representative of the disruption (Fig. 1). Regardless of the studied scenario, we weight the graph by using the travel times recorded at $7:30$ am when the impacts are the worst. The snowfall scenario (Fig. 1a), based on data from Monday 18^{th} 2017, hugely impacts the average speed during the morning peak hours compared to a typical Monday; the subway disruption scenario (Fig. 1b), based on data from Tuesday 19^{th} 2017, also introduces a speed reduction during the whole day compared to a typical Tuesday. The observed speed reduction may be due to the modal shift from the disrupted public transportation system towards privately owned vehicles which might have generated congestion on the road network. Finally, as the ultimate goal of the P&R system is to be competitive either during the week days or during week-ends, we consider two stochastic scenarios representing each kind of day (Fig. 1c). The probability depends on the scenario. We assumed the snowfall has similar impact to a rainfall and fix the probability of occurrence of 35%. The subway disruption could model more generally a public transport failure, which is a rather regular event. We fix the probability to 30%. Finally the

Algorithm 7: Swap search

Input: LB^n, $\boldsymbol{y}^{*,n}$
Output: LB^n, $\boldsymbol{x}^{*,n}$, $\boldsymbol{y}^{*,n}$, $\boldsymbol{x}$, $\boldsymbol{y}$

```
update ← True
while update = True do
    update ← False
    for i ∈ P ∪ D do
        ȳ ← y^{*,n}
        if y_i^{*,n} = 1 then
            ȳ_i ← 0
            for j ∈ P ∪ D do
                if y_j^{*,n} = 0  &  c_j^{loc} < c_i^{loc} then
                    ȳ_j ← 1
        else
            ȳ_i ← 1
            for j ∈ P ∪ D do
                if y_j^{*,n} = 1 then
                    ȳ_j ← 0
        x̄ ← Feasible flow for the park design ȳ (1) Algorithm 3
        LB̄ ← Compute the objective function for (x̄, ȳ) (5a)
        if LB̄ ≥ LB^n then
            LB^n ← LB̄
            (x^{*,n}, y^{*,n}) ← (x̄, ȳ)
            update ← True
            break
```

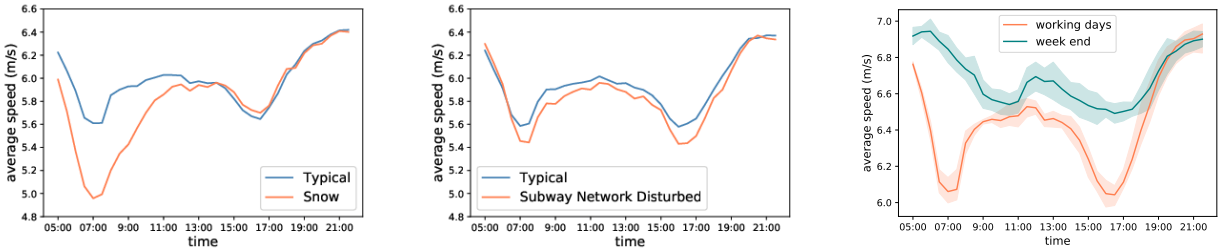

(a) Snowfall (b) Subway disruption (c) Working days and week-end

Figure 1: Average speeds observed at 7:30am are used to generate the four stochastic scenarios (snowfall (a), subway disruption (b), working and week-end days (c)).

probability for the normal week day (resp. week end day) is set to 25% (resp. 10%). Regarding the demand d^{ω}_{rs}, we use realistic data reconstructed by Krug et al. (2021) by relying on a methodology combining survey-based information, simulations and measures of flows collected via loop detectors installed in the city of Lyon. Moreover, demand data have been properly adapted, via an aggregation procedure, to the specific graph sizes considered in our evaluation (Sec. 6.1.1).

The construction cost c^{loc}_i for the pick up nodes corresponds to the cost that is required for a car park to be built, whereas the construction cost for drop off nodes corresponds to that of a transit stop. Hence, in our numerical experi-

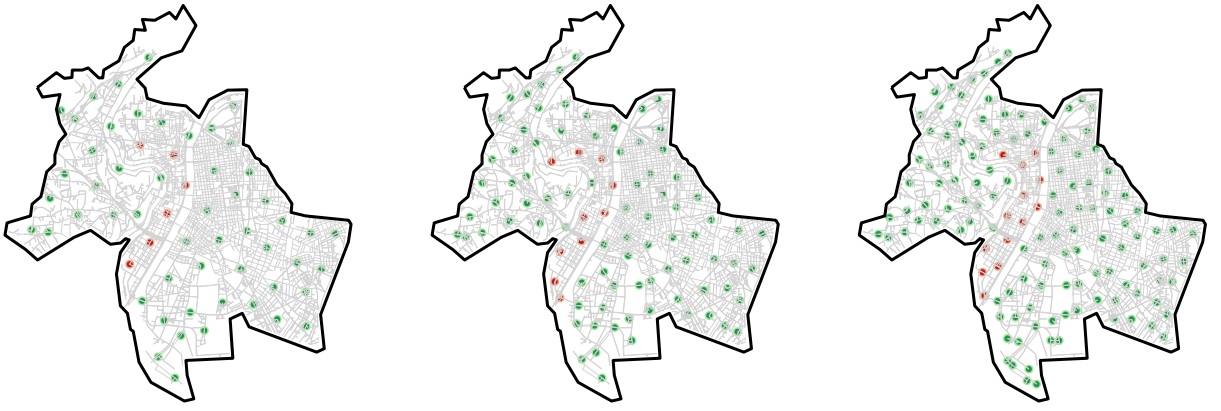

(a) 59 nodes (b) 93 nodes (c) 135 nodes

Figure 2: Reduced graphs with a given number of nodes where the green nodes are origins (potential pick ups) and the red nodes are the destinations (potential drop offs).

ments the construction cost of pick up nodes is chosen about ten times greater than that of drop off nodes. The budget allocated to the facility location construction B is defined as a percentage of the total cost corresponding to the opening of all the facility locations. In both sensitivity and real analysis, we use four different budgets corresponding to 20%, 40%, 60% or 80% of the total construction cost.

5.2. Experiments design

We implement the proposed P&R facility location formulations to instances based on the city of Lyon: trip generalized costs g^{ω}_{rijs} are determined based on the travel cost components $c^{\mathsf{R}_{rs},\omega}_{rs}$ and $c^{\text{access},\omega}_{ri}$, $c^{\text{route},\omega}_{ij}$, c^{walk}_{js}; the demand d^{ω}_{rs} and the construction cost of the pick ups and the drop offs c^{loc}_{i}. We conduct two analyses: a sensitivity analysis to measure the performance of the proposed LRA approach versus a direct MILP approach, and a real case study analysis to illustrate the behavior of the proposed P&R system in an operative context. We only consider the morning peak hour. For the evening commute, the role of pick ups and drop offs will be reversed.

For the sensitivity analysis, we consider three graph sizes: a small graph (S) composed of 59 nodes, which represents both potential pick ups and potential drop offs, a medium graph (M) composed of 93 nodes and a large graph (L) composed of 135 nodes (see Table 2). We aim at considering a restricted number of nodes of the road network, evenly distributed in Lyon. Therefore, we divide Lyon in equal areas using a spatial clustering method and assume that there is a unique origin (resp. destination) in each area which acts as a potential pick up (resp. drop off) based on its location in Lyon. For these instances (see Fig. 2a-2c), the set of origins (resp. destinations) is equal to the set of the potential pick ups P (resp. drop offs D). The green nodes represent the origins and the potential pick ups whereas the red nodes correspond to the destinations and the potential drop offs.

For the realistic case study, we assume that the set of origins (resp. destinations) differs from the set of potential pick ups (resp. drop offs) (see Fig. 3b). We use a segmentation of the city into zones, called Iris sectors (see Fig. 3a), developed by the French Institute of Statistics. Iris sectors divide the conurbation of Lyon into small geographical areas, each grouping approximately 2 000 inhabitants[3]. These areas are thus used to uniformly distribute the sets of potential pick ups and drop offs nodes in the graph. We assume that there is a unique potential pick up (resp. drop off) per Iris sector, which is the closest node to the centroid of the area. Concerning origin and destination nodes, they correspond to a tenth of the road intersection nodes of the real road network of Lyon, and they are uniformly distributed over the Lyon's city network.

The proposed formulations and algorithms are implemented in Python on a machine with 16 Gb of RAM and a CPU of 4.20GHz (Intel(R) Core(TM) i7-7700K). All mixed-integer and/or linear programs are solved using CPLEX's

[3] https://www.insee.fr/fr/metadonnees/definition/c1523

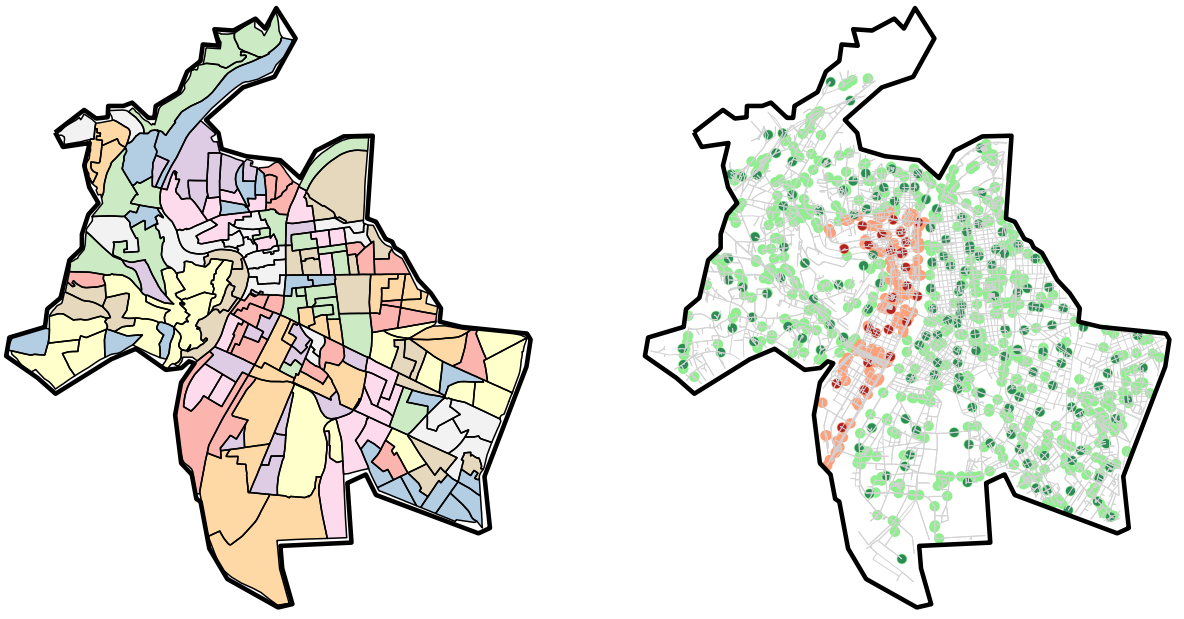

(a) Iris areas (b) Real graph

Figure 3: Iris areas (a): territory divisions encompassing 2 000 inhabitants. Network used for the real instance I^R (b): origins (light green), destinations (light red), potential pick ups(dark green) and potential drop offs (dark red).

	Small (S)	Medium (M)	Large (L)	Real (R)
Origins	53	83	121	745
Pick ups (P)	53	83	121	155
Drop offs (D)	6	10	14	25
Destinations	6	10	14	171

Table 2
Graph sizes description

Python API.

6. Results

In this section, we conduct numerical experiments to explore the behavior of the proposed P&R facility location formulations and compare the performance of the proposed Lagrangian Relaxation Algorithm (LRA) with a direct MILP approach.

6.1. Sensitivity analysis

The following results aim to showcase the ability of the proposed LRA to provide results that are superior to those obtained using a direct MILP solver for solving Formulation (5). We first examine the influence of the graph size (S, M, L) and the budget B (20%, 40%, 60%, 80%) on both solution methods (Sec. 6.1.1). In a second analysis, we explore the impact of the access time t^{access} and the egress time t^{egress} which determine the set of accessible pick ups from the origins and the set of drop offs allowing to access the destinations, respectively (Sec. 6.1.2). Finally, we observe the impact of the waiting time related to our P&R on the ridership. These parameters directly impact the

	Parameters		MILP			LRA			
Instance	t^{access}	t^{egress}	Budget (%)	Objective	Gap (%)	LB	Gap (%)	# Iterations	Gain (%)
I_1^S	3	10	20	1 053.850	4.6	1 001.849	25.2	237	-5.2
			40	1 189.682	3.8	1 181.146	12.4	259	-0.7
			60	1 241.595	1.5	1 235.390	9.6	253	-0.5
			80	1 259.218	0.0	1 257.202	8.1	261	-0.2
I_1^M	3	10	20	137.546	100.0	1 219.896	13.4	24	88.7
			40	1 257.042	6.3	1 289.893	8.4	24	2.5
			60	1 319.766	1.3	1 315.126	6.6	27	-0.3
			80	1 331.724	0.4	1 333.122	5.4	22	0.1
I_1^L	3	10	20	405.012	100.0	1 329.833	12.2	5	69.5
			40	-	-	1 400.280	7.6	5	-
			60	-	-	1 435.024	5.3	4	-
			80	1 455.080	0.3	1 450.163	4.3	4	-0.3

Table 3
Sensitivity analysis results after 1 hour running for the I_1 with an access time t^{access} and an egress time t^{egress} fixed to 3 and 10 minutes.

number of constraints in the formulations and may thus significantly influence the computational performance of the solution methods tested.

To perform our sensitivity analyses, we use a time limit of one hour. We analyze two different instances, named I_1 and I_2. The first instance I_1, is built on the construction cost randomly defined in the range of a car park construction or the transit stop installation, the travel time recorded in the FCD and the demand modified in accordance with the travel time variations during four specific days to define our four different stochastic scenarios: one Sunday, one Saturday, Christmas day and one Thursday. The second instance I_2, is also composed by construction cost, demand and travel times recorded by the FCD during other four different days: one Tuesday, one Monday, one day during the school holidays and one day during a city-center event in Lyon. By extracting the recorded travel time from the FCD (Sec. 5.1) and by adapting the recorded data to the three graph sizes (S, M, L) (Sec. 5.2) we create six instances I_1^S, I_2^S, I_1^M, I_2^M, I_1^L and I_2^L, with their own travel costs ($c_{ri}^{access,\omega}$, $c_{ij}^{route,\omega}$, c_{js}^{walk} and $c_{rs}^{R_{rs},\omega}$), demands (d_{rs}^{ω}) and construction costs c_i^{loc}). For the purpose of the sensitivity analysis, we decided to assign an equal probability of occurrence to each scenario.

6.1.1. Graph size

To analyze the impact of the graph size on the performance of the solution methods, we set t^{access} and t^{egress} to 3 minutes and 10 minutes, respectively. This means that the pick up must be reachable within a travel time of 3 minutes by a car from its origin and the drop off must be within a distance of 900 meters from the destination, to respect a maximum walking time constraint of 10 minutes. With such parameters, Formulation (5) leads to a problem with, on average, 267 000 constraints and 15 000 variables (binary and continuous) for the small graph size S, 2 000 000 constraints and 67 000 variables for the medium one M, and 15 000 000 constraints and 270 000 variables on the the large graph size L.

Tables 3 and 4 summarize the results obtained using the MILP approach and the proposed LRA algorithm for instances I_1 and I_2, respectively. We compute the LRA-gap as the relative gap between the upper and the lower bounds ($100 \times (\text{UB} - \text{LB})/\text{UB}$). Notably, the gap obtained using LRA is for some instances greater than the MILP gap even though both methods found comparable solutions in terms of objective value. This is because the Lagrangian relaxation duality gap cannot be guaranteed to be zero (Fisher, 2004). This occurs especially for the small graph size S where our lower bound often exceeds the best bound of the MILP approach. Conversely, we occasionally observe a lower MILP gap compared to the LRA gap but the MILP solution has a lower objective value than the best LB found using LRA. To compare the obtained feasible solutions, most of time sub-optimal, using the MILP approach and the LRA, we compute the gain as the relative gap between both solutions ($100 \times (\text{LB} - \text{Objective})/\text{LB}$). Note that the optimality gaps of both methods (MILP and LRA) may not reflect accurately the quality of the solutions obtained. A

	Parameters			MILP			LRA		
Instance	t^{access}	t^{egress}	Budget (%)	Objective	Gap (%)	LB	Gap (%)	# Iterations	Gain (%)
I_2^S	3	10	20	1 005.633	1.2	971.167	25.2	295	-3.5
			40	1 164.179	1.9	1 147.485	12.5	318	-1.4
			60	1 213.253	1.8	1 212.745	9.0	312	-0.0
			80	1 234.696	3.0	1 234.311	7.7	317	-0.0
I_2^M	3	10	20	386.739	100.0	1 163.132	17.4	33	66.7
			40	1 199.063	10.1	1 265.998	10.1	35	5.3
			60	1 295.332	2.1	1 297.806	7.9	31	0.2
			80	1 315.854	5.0	1 316.831	6.5	29	0.1
I_2^L	3	10	20	-	-	1 277.515	15.7	5	-
			40	1 234.430	17.4	1 382.467	8.7	5	10.7
			60	-	-	1 426.541	5.8	6	-
			80	1 443.765	0.4	1 443.189	4.7	6	-0.0

Table 4
Sensitivity analysis results after 1 hour running for the I_2 with an access time t^{access} and an egress time t^{egress} fixed to 3 and 10 minutes.

positive gain means that our lower bound is higher than the MILP solution. In this case, the gain is written in green and prove the ability of the proposed LRA to provide a better solution. Else, the gain is written in red.

On the small graph S, the proposed LRA is less efficient than the direct MILP approach (Tab. 3): the gain is negative for all instances and ranges from -5.2% for a budget of 20% to -0.2% for the larger budget 80%. We find that the proposed LRA is not particularly efficient for the small graph S and the lower budget 20% with a gap between the upper and the lower bounds of 25.2%. Nonetheless, for the medium M and the large L graph sizes, the proposed LRA is competitive relative to the MILP approach. For the first instance I_1 (Tab. 3) (resp. second instance I_2, Tab. 4), the gain is positive for all the budgets except for the one of 40% (I_1^M) (resp. all the budgets (I_2^M)) for the medium graph size M. Moreover this gain is very high, 88.7% for I_1^M and 66.7% for I_2^M for the lower budget of 20%. For the large graph size L, the gain is positive for the budget going from 20% to 60%. For both instances, the MILP approach is unable to provide a solution in one hour for two budgets tested (40% and 60% for I_1^L and 20% and 60% for I_2^L). Regardless of the graph size (S, M, L) and the instance (I_1 and I_2), the lower the budget, the higher the LRA gap due to the complexity of the problem (see Fig. 4). For all the graph sizes (S, M, L), we obtained a gap greater than 10.0% and most of time greater than 20.0% where the budget is 20% which is not particularly conclusive, although this is due to the slow reduction of the upper bound. Using a greater budget (40%, 60%, 80%) tends to reduce the optimality gap of the proposed LRA. This behavior can be explained by the fact that the initial upper bound, which is mostly the better one due to the slow even non-existent decrease during the one-hour allowed runtime, is equal to the portion of passengers using the P&R system when all the pick ups and drop offs are open. With a larger budget, more and more locations are open and the P&R's ridership rises, thus reducing the LRA gap with the upper bound.

The reported results clearly highlight an important limitation of the proposed LRA in the upper bound computation. Indeed, this bound is supposed to decrease through the iterations thanks to the evolution of the LM coefficients. Nonetheless, such decrease is only observed for the small graph size S, composed of 59 nodes, where a significantly higher number of iterations, more than 200, is performed within the allowed run-time constraint of one hour. Nonetheless, the lower bound rises across the iterations for all the budgets (20%, 40%, 60%, 80%) and the graph sizes (S, M, L), reducing the LRA-gap between the upper and lower bounds, proving the efficiency of the proposed LRA.

Figure 4 confirms these observed results and claims. For both instances, the gap between the proposed LRA based lower and upper bounds is larger when the budget is 20% for all the graph sizes (S, M, L) tested. The curves decrease significantly when the budget is equal to 40% and again when it is equal to 60%. Between 60% and 80% the decrease becomes more steady.

6.1.2. Impact of access time (t^{access}) and egress time (t^{egress}) on the model solving

The modification of t^{access} and t^{egress} highly influences the complexity of the problem by significantly increasing the number of constraints and decision variables of the model. With the small graph size S, the number of constraints

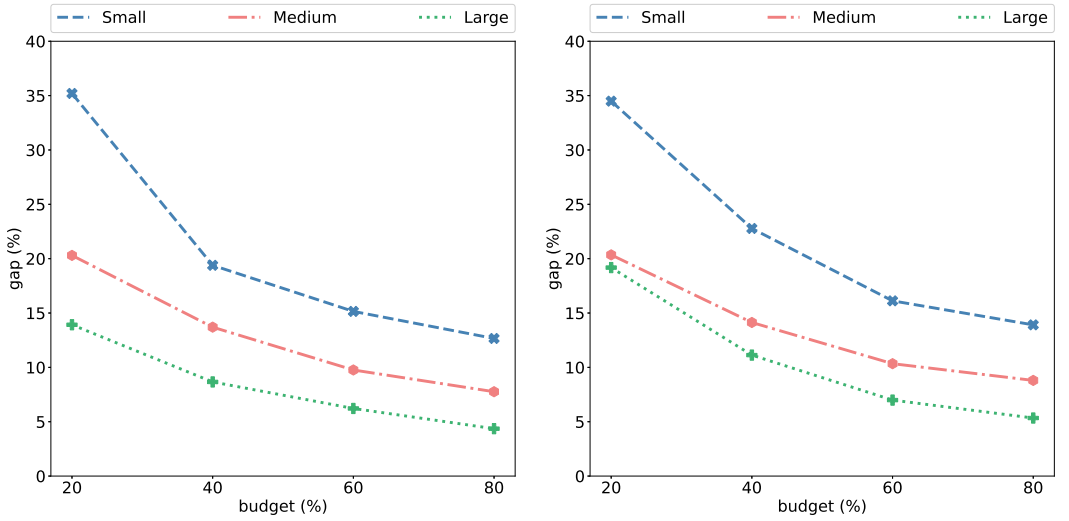

(a) 1^{st} instance I_1 (b) 2^{nd} instance I_2

Figure 4: Evolution of the gap between the Upper and Lower Bounds (UB and LB) computed with the proposed Lagrangian Relaxation Algorithm (LRA) for varying budget (20%, 40%, 60%, 80%). Results are reported for both instances I_1 and I_2 and for all three graph size (Small (S), Medium (M), Large (L)). In this computation, the access and egress parameters are set to $t^{\text{access}} = 3$ minutes and $t^{\text{egress}} = 10$ minutes.

	Parameters			MILP			LRA		
Instance	t^{access}	t^{egress}	Budget (%)	Objective	Gap (%)	LB	Gap (%)	# Iterations	Gain (%)
I_1^S	5	15	20	1 213.533	13.4	1 312.649	6.6	13	7.5
			40	1 351.306	1.8	1 355.782	3.5	14	0.3
			60	1 367.905	0.6	1 368.623	2.6	12	0.0
			80	1 374.490	0.1	1 372.509	2.3	14	-0.1
I_1^M	5	15	20	-	-	1 362.338	3.3	3	-
			40	-	-	1 379.385	2.1	2	-
			60	-	-	1 386.546	1.6	2	-
			80	-	-	1 390.005	1.3	2	-
I_1^L	5	15	20	-	-	1 478.955	-	-	-
			40	-	-	1 493.202	-	-	-
			60	-	-	1 496.828	-	-	-
			80	-	-	1 498.430	-	-	-

Table 5
Sensitivity analysis results for instance I_1 with a time limit of 1 hour with an access time t^{access} and an egress time t^{egress} fixed to 5 and 15 minutes.

increases of 1 500% and the number of variables rises of 450%. For the medium graph size M, the number of constraints increases of 1 750% and the number of variables rises also by 450%. For the large graph size L the direct MILP approach fails to be successfully implemented and CPLEX is unable to provide the number of constraints and variables for these instances. Table 5 presents the results obtained using the MILP approach and the proposed LRA with t^{access} equal to 5 minutes and t^{egress} equal to 15 minutes for the first instance I_1 and Table 6 shows the results for the second instance I_2. Contrary to the results for t^{access} and t^{egress} respectively equal to 3 and 10 minutes (Tab. 3 and 4), even for the small graph size S, the proposed LRA exhibits a better performance relatively to the MILP approach for a budget of 20%. Because of the complexity of the problem with the one-hour time constraints and the large graph size L, we

	Parameters		MILP			LRA			
Instance	t^{access}	t^{egress}	Budget (%)	Objective	Gap (%)	LB	Gap (%)	# Iterations	Gain (%)
I_2^S	5	15	20	-	-	1 302.943	7.3	17	-
			40	1 346.282	1.8	1 348.614	4.0	20	0.2
			60	1 362.894	0.6	1 358.044	3.4	23	-0.4
			80	1 368.242	0.2	1 368.312	2.6	24	0.0
I_2^M	5	15	20	-	-	1 338.419	5.0	4	-
			40	-	-	1 376.012	2.3	3	-
			60	-	-	1 382.271	1.9	3	-
			80	1 373.301	1.1	1 386.093	1.6	2	0.9
I_2^L	5	15	20	-	-	1 468.108	-	-	-
			40	-	-	1 491.181	-	-	-
			60	-	-	1 498.100	-	-	-
			80	-	-	1 500.114	-	-	-

Table 6
Sensitivity analysis results for instance I_2 with a time limit of 1 hour with an access time t^{access} and an egress time t^{egress} fixed to 5 and 15 minutes.

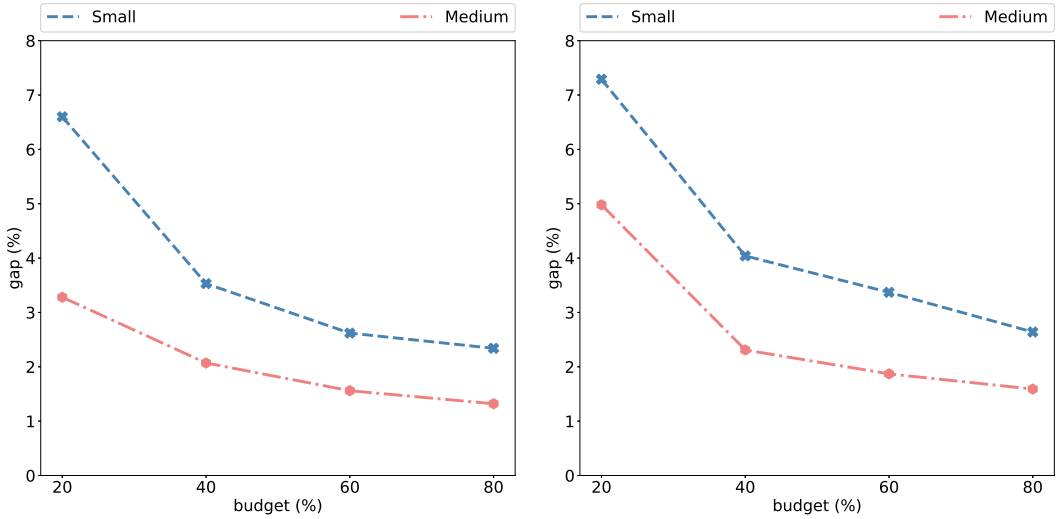

(a) 1^{st} instance I_1 (b) 2^{nd} instance I_2

Figure 5: Evolution of the gap between the Upper and Lower Bounds (UB and LB) computed with the proposed Lagrangian Relaxation Algorithm (LRA) for varying budget (20%, 40%, 60%, 80%). Results are reported for both instances I_1 and I_2 and for two graph size (Small (S), Medium (M)). In this computation, the access and egress parameters are set to $t^{access} = 5$ minutes and $t^{egress} = 15$ minutes.

are unable to solve Formulation (5) using a direct MILP. Solving the Lagrangian relaxation formulations (7) or (8) is also impossible in the one-hour time constraints for the large graph size. Nonetheless, the first heuristic (Alg. 2) developed in the LRA successes to provide a lower bound to the problem which is a feasible solution. The quality of this solution cannot be assessed due to the lack of an upper bound. For the medium graph size M (Tab. 2), the direct MILP approach is unable to find a feasible solution, except for I_2^M and a budget of 80%, whereas the LRA provides a solution whose gaps do not exceed 5.0% for all the considered budget values.

Figure 5 provides insights about the accuracy of our algorithm. Regarding these results, we can conclude that except for a budget of 20% computed with the small graph size S (I_1^S and I_2^S), the gap between the bounds is globally

		LB				P&R flow share			
	Budget (%)	0min	+5min	+10min	+15min	0min	+5min	+10min	+15min
I^S	20	963.5	972.4	964.7	952.3	66.9%	66.0%	66.2%	64.7%
	40	1 147.3	1 157.5	1 145.7	1 124.8	78.1%	78.6%	77.8%	70.8%
	60	1 249.6	1 246.0	1 238.2	1 239.4	84.6%	82.4%	80.9%	81.5%
	80	1 286.2	1 282.1	1 276.4	1 271.1	86.7%	86.7%	86.3%	86.3%
I^M	20	1 055.5	1 059.8	1 054.8	1 049.7	78.8%	72.6%	77.8%	75.8%
	40	1 147.6	1 145.8	1 141.9	1 137.9	86.6%	84.0%	75.7%	76.2%
	60	1 194.7	1 197.1	1 193.8	1 190.5	90.2%	87.6%	87.3%	87.0%
	80	1 221.9	1 220.2	1 217.4	1 214.5	91.7%	91.7%	91.3%	91.3%
I^L	20	1 1973.6	1 1943.7	1 1913.1	11 881.9	84.9%	82.6%	85.0%	84.7%
	40	1 2771.0	1 2744.3	12 716.9	12 688.9	92.2%	92.1%	91.9%	91.7%
	60	1 3043.3	1 3077.2	13 056.5	13 043.0	93.0%	93.3%	93.1%	92.8%
	80	1 3303.1	1 3286.0	13 268.3	13 250.3	95.8%	95.4%	95.2%	95.4%

Table 7
Sensitivity analysis on the waiting time of P&R mobility alternatives.

lower than 5.0% and thus truly close to the optimal solution.

6.1.3. Impact of the P&R system waiting time

We next conduct a sensitivity analysis on the attractiveness of P&R mobility alternatives by incorporating user waiting time within the corresponding generalized costs. Specifically, we inflate the generalized costs of P&R alternatives by adding a waiting time ranging from 5 to 15 minutes. The results of this analysis are summarized in Table 7. As expected, a longer waiting time tends to lower the percentage of users choosing the P&R system. Nonetheless, the differences are very marginal, with the only exception of the case where the budget is fixed to 40% of the maximal one between both extreme waiting times (0 minute and +15 minutes): in this case, the reduction of users is about 7.3% for the small graph size, 10.4% for the medium one, and only 0.4% for the large one. For all the other budgets and graph sizes, the difference induced by the waiting time increase is always lower, not exceeding 4% between both extreme waiting times (0 minute and +15 minutes).

In conclusion, the sensitivity analysis highlights the potential of our solution with larger t^{access} and t^{egress} times, in terms of the larger size of the problem that we are able to solve. Similarly, larger percentages of construction cost budgets underline the ability of our LRA solution to outperform the commercial MILP solver by providing a competitive solution for all the percentage range. Regarding the following realistic analysis, we focus instead on smaller budgets, comprised between 5% and 20%, because of the consistency of the flow share with the reality.

6.2. Realistic case study

In this section, we present results computed on a realistic graph size (R) composed of 746 origins and 171 destinations with 155 potential pick ups and 25 potential drop offs. The set of potential pick ups and drop offs is uniformly distributed across the network geography and the population spreading. Specifically, we determine a potential pick up or drop off per Iris area (Sec. 5). The access and egress times are respectively fixed at $t^{\text{access}} = 2$ minutes and $t^{\text{egress}} = 8$ minutes. Such problem is composed of about 9 062 000 variables and induced around 77 000 constraints. We customize the proposed LRA in order to balance the time assigned to the local search heuristics and the number of realized iterations in one hour of runtime. The time dedicated to the local search heuristics (Alg. 6 and Alg. 7) is fixed at 20 minutes per iteration rather than 10 minutes per iteration in the sensitivity analysis (Sec. 6.1).

Table 8 summarize the results obtained with the realistic instance for access times fixed to 2 minutes and egress times equal to 8 minutes. The sensitivity parameter to the generalized cost θ is equal to 0.1 as in the sensitivity analysis. Whatever the allocated budget (5%, 10%, 15% and 20%), the LRA always exceeds the MILP approach performances by always providing an higher feasible solutions. For the smallest budget, the gain between both solutions even exceeds 50%. Although the gap of the LRA is important due to the small reduction of the upper bound, the lower bound, representing the best found feasible solution, is very interesting to solve the complex problem of allocating P&R, respecting a market share model, on a large-scale network.

Table 9 summarizes the flow shares using the P&R for an access time fixed at 2 minutes and an egress time set to 8

			Parameters	MILP		LRA		
Instance	t^{access}	t^{egress}	Budget (%)	Objective	Gap (%)	LB	Gap (%)	Gain (%)
I^R	2	8	5	287.956	2.9	902.346	51.5	68.1
			10	1 156.906	0.3	1 352.844	27.3	14.4
			15	1 408.596	0.2	1 534.226	17.6	8.1
			20	1 618.571	0.0	1 618.593	13.0	0.0

Table 8
Real instance results after 1 hour running for the first instance I_1 with an heuristic time constraint of 20 minutes and with the first lower bound LB^0 computation (Alg. 2). The access time t^{access} and the egress time t^{egress} are fixed to 2 and 8 minutes and the generalized cost sensitivity θ is set to 0.1.

		Scenario	P&R flow share			
Index	Description	Prob.	Budget 5%	Budget 10%	Budget 15%	Budget 20%
0	Snowfall / heavy rainfall impact	0.35	42.67%	67.41%	76.84%	86.35%
1	Public transport disruption	0.30	46.95%	75.78%	82.70%	86.90%
2	Week day	0.25	54.82%	72.05%	86.25%	88.98%
3	Week-end	0.1	44.33%	69.56%	78.65%	82.79%

Table 9
$\theta = 0.1$, $t^{\text{access}} = 2$ minutes, $t^{\text{egress}} = 8$ minutes

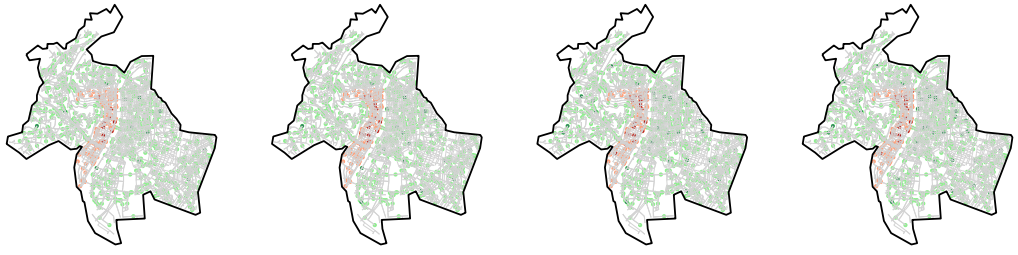

(a) 5%: 12 P and 10 D (b) 10%: 20 P and 15 D (c) 15%: 29 P and 20 D (d) 20%: 37 P and 20 D

Figure 6: Real instance with a given number of nodes where the green nodes are origins (potential pick ups) and the red nodes are the destinations (potential drop offs) for an access time fixed at 2 minutes and an egress one set to 8 minutes with $\theta = 0.1$.

minutes, depending on the allocated budget to the facilities construction and the scenario. The higher the the budget, the more people use the P&R due to the increase of possible path alternatives induced by the rise of the open pick ups and drop offs (Fig. 6), reducing the travel cost of the P&R mode by being closer to both origin and destination. We notice the P&R is fitted to recurrent disruptions by being highly attractive even in presence of snowfall or public transport disruption. Although the flow share is not equal for all the scenarios, the order of magnitude remains the same.

An increase of acces and egress times leads to a rise of the attractiveness for the P&R by serving a larger part of the demand for the same allocated budgets. This observation has been confirmed for and egress times respectively fixed to 3 and 10 minutes. Whereas, for a construction budget of 5% (resp. 20%), in average 47.91% (resp. 86.25%) of users choose the P&R system with and egress times fixed at 2 and 8 minutes, 61.73% (resp. 92.71%) of people use the P&R system for and egress times set to 3 and 10 minutes. By being larger, the access and egress times make P&R alternatives accessible to more origins and more destinations increasing the part of the demand served by the transport service with a similar number of opened pick ups and drop offs. For this greater pair of access and egress time, the MILP approach is unable to provide solution contrary to our LRA.

			Parameters	MILP		LRA		
Instance	t^{access}	t^{egress}	Budget (%)	Objective	Gap (%)	LB	Gap (%)	Gain (%)
I^R	2	8	5	116.441	7.1	679.262	63.5	82.8
			10	444.019	1.9	1 050.090	43.6	57.7
			15	545.510	1.6	1 271.339	31.7	57.1
			20	1 379.869	0.1	1 374.214	26.1	0.0

Table 10
Real instance results after 1 hour running for the first instance I_1 with an heuristic time constraint of 20 minutes and with the first lower bound LB^0 computation (Alg. 2). The access time t^{access} and the egress time t^{egress} are fixed to 2 and 8 minutes and the generalized cost sensitivity θ is set to 1.

		Scenario	P&R flow share			
Index	Description	Prob.	Budget 5%	Budget 10%	Budget 15%	Budget 20%
0	Snowfall / heavy rainfall impact	0.35	35.70%	54.98%	64.19%	73.02%
1	Public transport disruption	0.30	36.16%	55.75%	67.24%	72.75%
2	Week day	0.25	40.18%	58.97%	73.57%	77.54%
3	Week-end	0.1	39.13%	53.29%	65.81%	71.69%

Table 11
$\theta = 1$, $t^{access} = 2$ minutes, $t^{egress} = 8$ minutes

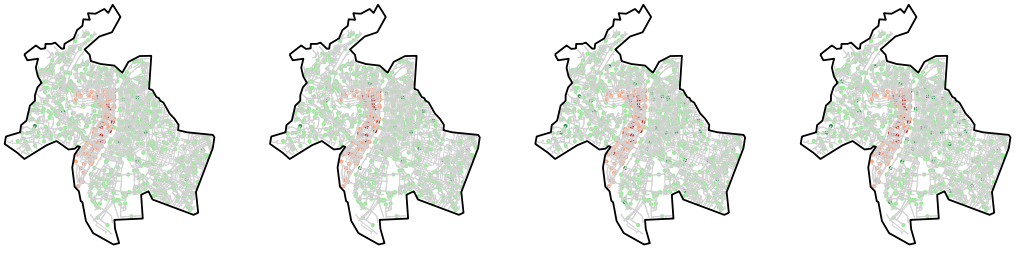

(a) 5%: 11 P and 11 D (b) 10%: 18 P and 20 D (c) 15%: 29 P and 20 D (d) 20%: 38 P and 20 D

Figure 7: Real instance with a given number of nodes where the green nodes are origins (potential pick ups) and the red nodes are the destinations (potential drop offs) for an time fixed at 2 minutes and an egress one set to 8 minutes with $\theta = 1$.

6.2.1. Sensitivity with respect to the generalized cost in the market share model ($\theta = 1$)

In this analysis, we measure the impact of parameter θ (sensitivity to the generalized cost in the mobility choice model) by increasing it from 0.1 to 1. By observing the results obtained in such conditions (Table 10), we notice that whatever the budget and the and egress times, the lower bounds, corresponding to the best feasible solutions, are always lower than the ones obtained with a smaller θ (Table 8). The P&R system is less attractive when the sensitivity to the generalized cost is increased, due to the longer travel cost induced by the consideration of a walking travel time part, between the drop off and the destination, in the P&R path.

The flow share distributions (Tab. 11) confirm this decrease in the usage of the P&R system with the increase of the generalized cost sensitivity. Whereas on average 47.91% (resp. 86.25%) of people use the P&R system for an access time set to 2 minutes, an egress time fixed to 8 minutes and a budget for the construction limit to 5% (resp. 20%) of the global construction cost with a θ parameter equal to 0.1, with the increase in generalized cost sensitivity ($\theta = 1$), only 37.79% (resp. 73.75%) of people choose the P&R system to travel. Similar trends are observed with higher budgets.

7. Conclusion and perspectives

In this study, we proposed a new approach for locating P&R facilities to enhance the resilience of urban mobility networks. By proposing an on-demand P&R system and by maximizing the ridership of the P&R system in the presence of recurrent disruptions, we aim at reducing the use of private vehicle over the network which are often the source of congestion in mobility networks. With the establishment of such a new public transport mode we reduce the number of vehicles over the network for a same amount of travelers. Thus, by capturing a part of the demand, the P&R system is expected to improve the resilience of the mobility network to recurrent traffic disruptions. Our rationale is that using the model outputs, *i.e.*, scenario-based OD route flow shares x^{ω}_{rijs}, the decision-maker can determine the expected number of users on a transit route as $d^{\omega}_{rs} \times x^{\omega}_{rijs}$. This expected route flow can then be used to plan for shuttle deployment. Although the integration of shuttle and maintenance costs in the problem formulation might increase the level of detail from an operational standpoint, the proposed model aims to inform decision-making at a strategic level. We leave the development of more operational formulations for future research. The proposed formulation aims to find optimal location for pick up and drop off facilities. These P&R facilities are used to provide on-demand mobility services that complement the existing transport network. Users' trips in the P&R system are modeled as three-link chains, i.e. from origin to pick up, drop off and destination. Users' modal shift from reserve travel modes to the proposed P&R mobility service is modeled using a logit choice model and the goal is to maximize the expected ridership in the P&R system under varying traffic conditions. Specifically, we propose a stochastic programming approach where a set of finite scenarios is considered, which may represent both regular traffic conditions and recurrent disruptions in the network. The resulting P&R facility location formulation is a challenging mixed-integer linear programming (MILP) problem with a large number of decision variables. We develop a Lagrangian relaxation approach to solve large scale instances. We decompose the relaxed formulation into sub-problems that can be solved efficiently and propose local-search algorithms to find competitive solutions along the search.

We conduct extensive numerical experiments based on instances generated using real data from the urban transport network of Lyon, France. Across our numerical experiments, we observe that the complexity of the problem increases with the size of the graph and the decrease of the allocated budget for opening facilities in the P&R system. Compared to the direct MILP approach, the proposed Lagrangian Relaxation Algorithm (LRA) is more scalable and capable to generate feasible solutions with large-size instances. Although the optimality gap of the LRA is sometimes higher than that of the MILP approach, the LRA often finds better feasible solutions. The results obtained on the realistic instance (Sec. 6.2) proves the ability of the proposed LRA to provide information about the implementation of a budget constrained optimized P&R system adapted to the recurrent disruptions in a large-scale network. The results also insight about the flow share distribution between the reserve mode and the P&R for a given allocated budget. For larger budgets, the number of opened pick up and drop off facilities increases significantly. This leads to an increase in the number of feasible transit routes in the P&R system which results in relatively large flow shares for this mobility option compared to the reserve mode. While flow shares of this magnitude may be unrealistically high, this can be explained by the fact that only a single concurrent mobility mode is considered – the reserve mode – which may not be sufficient to fully capture competition effects across travel options in an urban multi-modal transportation network. Since the focus of our study is on developing optimization methods, we leave the detailed modeling of such mobility alternatives for future research.

This study has focused on the design of P&R systems with the aim to improve the resilience of urban mobility networks in presence of recurrent disruptions. However, the proposed facility location approach can be generalized beyond P&R systems to the design of flexible multi-modal and on-demand mobility networks. Indeed, the proposed framework could be used to model three-link trip chains in a generic context. Further research is also needed to incorporate fleet sizing and vehicle or line capacity in the proposed framework. The addition of the P&R system may influence transit flows and subsequently traffic congestion in the network. The incorporation of congestion effects in the proposed framework may be achieved by incorporating a traffic and/or transit assignment. Such extensions of the proposed formulation will be explored in future works.

References

, . Lagrangian Relaxation. Technical Report. URL: http://www.ens-lyon.fr/DI/wp-content/uploads/2012/01/LagrangianRelax.pdf.

Andrejszki, T., Torok, A., Csete, M., 2015. Identifyingy the utility function of transport services from stated preferences. Transport and Telecommunication 16, 138–144. doi:10.1515/ttj-2015-0013.

Angelo, G.D.., Severini, L., Velaj, Y., 2016. On the Maximum Betweenness Improvement Problem. Electronic Notes in Theoretical Computer Science 322, 153–168. URL: http://dx.doi.org/10.1016/j.entcs.2016.03.011, doi:10.1016/j.entcs.2016.03.011.

Annisa, A., Herman, H., Wiradinata, I., 2019. A sustainable transportation: a literature study on park and ride in the Bandung metropolitan area, in: International Conference on Advances in Civil and Environmental Engineering. URL: https://doi.org/10.1051/matecconf, doi:10.1051/matecconf/201927603008.

Aros-Vera, F., Marianov, V., Mitchell, J.E., 2013. p-Hub approach for the optimal park-and-ride facility location problem. European Journal of Operational Research 226, 277–285. URL: https://linkinghub.elsevier.com/retrieve/pii/S0377221712008223, doi:10.1016/j.ejor.2012.11.006.

Bababeik, M., Khademi, N., Chen, A., 2018. Increasing the resilience level of a vulnerable rail network: The strategy of location and allocation of emergency relief trains. Transportation Research Part E: Logistics and Transportation Review 119, 110–128. URL: https://www.sciencedirect.com/science/article/pii/S1366554517312358?casa_token=pahatptMxZOAAAAA:kB9yG-qGJ2GcQ0Q80Gp7I6vClDdlcdaSrd37xTQ2CHC5kS-jyGcd6c7D-mzgtS4ABNiE1fz97Nc, doi:10.1016/J.TRE.2018.09.009.

Basciftci, B., Van Hentenryck, P., 2020. Bilevel Optimization for On-Demand Multimodal Transit Systems, in: Lecture Notes in Computer Science (including subseries Lecture Notes in Artificial Intelligence and Lecture Notes in Bioinformatics), Springer Science and Business Media Deutschland GmbH. pp. 52–68. doi:10.1007/978-3-030-58942-4{_}4.

Berche, B., Von Ferber, C., Holovatch, T., Holovatch, Y., 2009. Resilience of public transport networks against attacks. Eur. Phys. J. B 71, 125–137. doi:10.1140/epjb/e2009-00291-3.

Bergamini, E., Meyerhenke, H., Crescenzi, P., 2018. Improving the Betweenness Centrality of a Node by Adding Links. Journal of Experimental Algorithmics 23. URL: https://arxiv.org/pdf/1702.05284.pdf.

Bíl, M., Vodák, R., Kubeček, J., Bílová, M., Sedoník, J., 2015. Evaluating road network damage caused by natural disasters in the Czech Republic between 1997 and 2010. Transportation Research Part A: Policy and Practice 80, 90–103. URL: https://www.sciencedirect.com/science/article/pii/S0965856415001883, doi:10.1016/J.TRA.2015.07.006.

Cavadas, J., Antunes, A.P., 2019. Optimization-based study of the location of park-and-ride facilities. Transportation Planning and Technology 42, 201–226. URL: https://www.tandfonline.com/doi/full/10.1080/03081060.2019.1576380, doi:10.1080/03081060.2019.1576380.

Chen, X., Kim, I., 2018. Modelling Rail-Based Park and Ride with Environmental Constraints in a Multimodal Transport Network. Journal of Advanced Transportation 2018, 1–15. URL: https://www.hindawi.com/journals/jat/2018/2310905/, doi:10.1155/2018/2310905.

Chen, X., Liu, Z., Currie, G., 2016. Optimizing location and capacity of rail-based Park-and-Ride sites to increase public transport usage. Transportation Planning and Technology 39, 507–526. URL: http://www.tandfonline.com/doi/full/10.1080/03081060.2016.1174366, doi:10.1080/03081060.2016.1174366.

Crescenzi, P., Severini, L., Velaj, Y., 2016. Greedily Improving Our Own Closeness Centrality in a Network. ACM Transactions on Knowledge Discovery from Data 11, 1–32. URL: https://hal.inria.fr/hal-01390134, doi:10.1145/2953882{\"{i}}.

Danach, K., Gelareh, S., Neamatian Monemi, R., 2019. The capacitated single-allocation p-hub location routing problem: a Lagrangian relaxation and a hyper-heuristic approach. EURO Journal on Transportation and Logistics 8, 597–631. URL: https://www.sciencedirect.com/science/article/pii/S2192437620300388, doi:10.1007/S13676-019-00141-W.

Donovan, B., Work, D.B., 2017. Empirically quantifying city-scale transportation system resilience to extreme events. Transportation Research Part C: Emerging Technologies doi:10.1016/j.trc.2017.03.002.

Du, B., Wang, D.Z., 2014. Continuum modeling of park-and-ride services considering travel time reliability and heterogeneous commuters – A linear complementarity system approach. Transportation Research Part E: Logistics and Transportation Review 71, 58–81. URL: https://www.sciencedirect.com/science/article/pii/S1366554514001483, doi:10.1016/J.TRE.2014.08.008.

Eusgeld, I., Kröger, W., Sansavini, G., Schläpfer, M., Zio, E., 2009. The role of network theory and object-oriented modeling within a framework for the vulnerability analysis of critical infrastructures. Reliability Engineering & System Safety 94, 954–963. URL: https://www.sciencedirect.com/science/article/pii/S095183200800263 9?via%3Dihub, doi:10.1016/J.RESS.2008.10.011.

Farahani, R.Z., SteadieSeifi, M., Asgari, N., 2010. Multiple criteria facility location problems: A survey. Applied mathematical modeling URL: https://reader.elsevier.com/reader/sd/pii/S0307904X09003242?token=331AA727E57B01A15D0FA3DECC8CF600B5B8FF22B2696FF3A2E73BB3298AF423AD09EF9F70405EF59CA154AEC115EEFF.

Farhan, B., Murray, A.T., 2008. Siting park-and-ride facilities using a multi-objective spatial optimization model. Computers & Operations Research 35, 445–456. URL: https://www.sciencedirect.com/science/article/pii/S0305054806000980, doi:10.1016/J.COR.2006.03.009.

Fischer, A., Niedermeier, M., Kokot, F., De Meer, H., Gorinsky, S., Papadimitriou, D., Karaliopoulos, M., Kuipers, F., Doerr, C., Shirazi, N., Knowles, W., Hutchison, D., Niedermayer, H., 2013. Overview on Methodology and Tools for Resilient Services. Technical Report. Information and Communication Technologies.

Fisher, M.L., 2004. The Lagrangian Relaxation method for solving integer programming problems. Management Science 50, 1861–1871. URL: https://my.eng.utah.edu/~kalla/phy_des/lagrange-relax-tutorial-fisher.pdf, doi:10.1287/mnsc.1040.0263.

Freiria, S., Ribeiro, B., Tavares, A.O., 2015. Understanding road network dynamics: Link-based topological patterns. Journal of Transport Geography 46, 55–66. URL: https://www.sciencedirect.com/science/article/pii/S0966692315000757?via%3Dihub, doi:10.1016/J.JTRANGEO.2015.05.002.

Gauthier, P., Furno, A., El Faouzi, N.E., 2018. Road network resilience: how to identify critical linkssubject to day-to-day disruptions? Transport Research Record .

Haimes, Y.Y., 2009. On the Definition of Resilience in Systems. Risk Analysis 29, 498–501. URL: http://doi.wiley.com/10.1111/j.1539-6924.2009.01216.x, doi:10.1111/j.1539-6924.2009.01216.x.

Hassan, S.M., Moghaddam, M., Bhouri, N., Scemama, G., 2019. Assessment of System Resilience: Robustness, Reliability and Redundancy of Public Transport Operation .

Henry, E., Furno, A., El Faouzi, N.E., Rey, D., 2021. Optimal Park-and-ride Facility Location and Fleet Sizing to Enhance the Resilience of Transport Networks, in: 8th International Conference on Transport Network Reliability. URL: https://www.transportenvironment.org/sites/te/files/publications/2019_09_Briefing_LEZ-ZEZ_.

Hitge, G., Vanderschuren, M., 2015. Comparison of travel time between private car and public transport in Cape Town. Journal of the South African Institution of Civil Engineering 57, 35–43. doi:10.17159/2309-8775/2015/v57n3a5.

Holling, C.S., 1973. Resilience of ecological systems. Source: Annual Review of Ecology and Systematics 4, 1–23. URL: http://www.jstor.org/stable/2096802http://www.jstor.org/stable/2096802http://www.jstor.org/stable/2096802.

Huang, K., Correia, G.H.d.A., An, K., 2018. Solving the station-based one-way carsharing network planning problem with relocations and non-linear demand. Transportation Research Part C: Emerging Technologies 90, 1–17. URL: https://linkinghub.elsevier.com/retrieve/pii/S0968090X18302511, doi:10.1016/j.trc.2018.02.020.

Jenelius, E., Cats, O., 2015. The value of new public transport links for network robustness and redundancy. Transportmetrica A: Transport Science 11, 819–835. URL: http://www.tandfonline.com/doi/full/10.1080/23249935.2015.1087232, doi:10.1080/23249935.2015.1087232.

Jian, S., Rey, D., Dixit, V., 2019. An Integrated Supply-Demand Approach to Solving Optimal Relocations in Station-Based Carsharing Systems. Networks and Spatial Economics 19, 611–632. doi:10.1007/s11067-018-9401-6.

Krug, J., Burianne, A., Bécarie, C., Leclercq, L., 2021. Refining trip starting and ending locations when estimating travel-demand at large urban scale. Journal of Transport Geography 93, 103041. URL: https://www.sciencedirect.com/science/article/abs/pii/S0966692321000946, doi:10.1016/J.JTRANGEO.2021.103041.

Lee, C., Nair, R., 2021. Robust transit line planning based on demand estimates obtained from mobile phones. EURO Journal on Transportation and Logistics 10, 100034. URL: https://www.sciencedirect.com/science/article/pii/S2192437621000066, doi:10.1016/J.EJTL.2021.100034.

Lee, Y.J., Vuchic, V.R., 2005. Transit Network Design with Variable Demand. Journal of transportation engineering URL: https://ascelibrary.org/doi/pdf/10.1061/%28ASCE%290733-947X%282005%29131%3A1%281%29, doi:10.1061/(ASCE)0733-947X(2005)131:1(1).

Lu, X., Wrathall, D.J., Sundsøy, P.R., Nadiruzzaman, M., Wetter, E., Iqbal, A., Qureshi, T., Tatem, A.J., Canright, G.S., Engø-Monsen, K., Bengtsson, L., 2016. Detecting climate adaptation with mobile network data in Bangladesh: anomalies in communication, mobility and consumption patterns during cyclone Mahasen. Climatic Change doi:10.1007/s10584-016-1753-7.

Machado, C.A., Hue, N.P.M.d.S., Berssaneti, F.T., Quintanilha, J.A., 2018. An overview of shared mobility. doi:10.3390/su10124342.

Mohring, H., 1972. Optimization and Scale Economies in Urban Bus Transportation. American Economic Review URL: https://www.jstor.org/stable/1806101?seq=1#metadata_info_tab_contents.

Murray-Tuite, P., 2006. A comparison of transportation network resilience under simulated System Optimum and User Equilibrium conditions. Proceedings of the 2006 Winter Simulation Conference doi:10.1145/1218112.1218367.

Noel, E.C., 1988. Park-and-Ride: Alive, Well, and Expanding in the United States. Journal of Urban Planning and Development 114, 2–13. URL: http://ascelibrary.org/doi/10.1061/%28ASCE%290733-9488%281988%29114%3A1%282%29, doi:10.1061/(ASCE)0733-9488(1988)114:1(2).

Oliveira, E.L.d., Portugal, L.d.S., Junior, W.P., 2014. Determining Critical Links in a Road Network: Vulnerability and Congestion Indicators. Procedia - Social and Behavioral Sciences 162, 158–167. URL: https://www.sciencedirect.com/science/article/pii/S1877042814062971, doi:10.1016/J.SBSPRO.2014.12.196.

Parkhurst, G., 1995. Park and ride: Could it lead to an increase in car traffic? Transport Policy 2, 15–23. doi:10.1016/0967-070X(95)93242-Q.

Ruan, J.M., Liu, B., Wei, H., Qu, Y., Zhu, N., Zhou, X., 2016. How Many and Where to Locate Parking Lots? A Space–time Accessibility-Maximization Modeling Framework for Special Event Traffic Management. Urban Rail Transit 2, 59–70. URL: http://link.springer.com/10.1007/s40864-016-0038-9, doi:10.1007/s40864-016-0038-9.

Shalaby, A., Eng, P., King, D., 2016. Performance Metrics and Analysis of Transit Network Resilience in Toronto. Transport Research Board .

Song, Z., He, Y., Zhang, L., 2017. Integrated planning of park-and-ride facilities and transit service. Transportation Research Part C: Emerging Technologies 74, 182–195. URL: https://linkinghub.elsevier.com/retrieve/pii/S0968090X16302418, doi:10.1016/j.trc.2016.11.017.

Sun, J., 2017. External Economic Costs of Intelligent Urban Transportation Systems: A Method to Evaluate the Externalities of Comparative Technology Adoption Pathways in the Urban Mobility Service sector. Technical Report. Clemson University. URL: https://tigerprints.clemson.edu/all_dissertations.

Tu, Y., Yang, C., Chen, X., 2010. Methodology for Evaluating and Improving Road Network Topology Vulnerability, in: 2010 International Conference on Intelligent Computation Technology and Automation, IEEE. pp. 664–669. URL: http://ieeexplore.ieee.org/document/5523334/, doi:10.1109/ICICTA.2010.603.

Zhang, L., Gu, W., Fu, L., Mei, Y., Hu, Y., 2021. A two-stage heuristic approach for fleet management optimization under time-varying demand. Transportation Research Part E: Logistics and Transportation Review 147, 102268. URL: https://www.sciencedirect.com/science/article/pii/S1366554521000442?casa_token=XKaXIh168vMAAAAA:MlPNfR7wVkWivppXng4RniGoPnykAatDWWe-_WrtEEkVuZA3hgpHCutn10Ny4_cDXnlr_wU5sp0, doi:10.1016/J.TRE.2021.102268.

Zhu, Y., Ozbay, K., Xie, K., Yang, H., 2016. Using Big Data to Study Resilience of Taxi and Subway Trips for Hurricanes Sandy and Irene. Transportation Research Record: Journal of the Transportation Research Board , 70–80doi:10.3141/2599-09.